# LANGMUIR

pubs.acs.org/Langmuir Article

# Oscillatory and Relaxation Study of the Interfacial Rheology of Star Polymers with Low-Grafting-Density PEO Arms and Hydrophobic Poly(divinylbenzene) Cores

Mateusz Olszewski, Xiaolei Hu, Ting-Chih Lin, Krzysztof Matyjaszewski,\* Natalia Lebedeva, and Philip Taylor\*



Cite This: Langmuir 2023, 39, 7741-7758



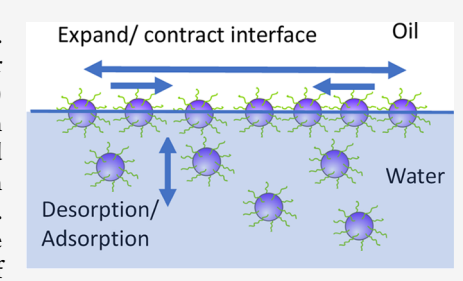
ACCESS |

III Metrics & More

Article Recommendations

Supporting Information

**ABSTRACT:** Star polymers have been gaining interest due to their tunable properties. They have been used as effective stabilizers for Pickering emulsions. Herein, star polymers were synthesized via activators regenerated by electron transfer (ARGET) atom transfer radical polymerization (ATRP). Poly(ethylene oxide) (PEO) with terminal  $\alpha$ -bromoisobutyrate ATRP functionality was used as a macroinitiator and divinylbenzene as a crosslinker for the arm-first star synthesis. Stars with PEO arms with a molar mass of either 2 or 5 kDa had a relatively low density of grafted chains, i.e., ca. 0.25 chain/nm². The properties of PEO stars adsorbed at oil—water interfaces were investigated using interfacial tension and interfacial rheology. The magnitude of interfacial tensions at oil—water interfaces depends on the nature of the oil phase, being



lower at the *m*-xylene/water interface than at the *n*-dodecane/water interface. Small differences were observed for stars with different molecular weights of PEO arms. The overall behavior of PEO stars adsorbed at an interface can be considered as an intermediate between a particle and a linear/branched polymer. Obtained results offer an important insight into the interfacial rheology of PEO star polymers in the context of their application as stabilizers for Pickering emulsions.

# ■ INTRODUCTION

The adsorption of nanoparticles at interfaces has been of increasing interest, especially in relation to their use as stabilizers for Pickering emulsions and their interfacial rheological properties.1-Such nanoparticles have been prepared by controlled radical polymerization methods such as atom transfer radical polymerization (ATRP).8-14 ATRP techniques have been employed to prepare hairy nanoparticles of variable dimensions, including star polymers of a size of a few nanometers. Stars can be synthesized by core-first or arm-first approach. The latter method can employ hydrophilic arms, such as poly(ethylene oxide) (PEO) with terminal  $\alpha$ -bromoisobutyrate ATRP functionality to be used as macroinitiators. Such macroinitiators can be then crosslinked by divinylbenzene (DVB) to generate a hydrophobic core of the resulting star with hydrophilic PEO arms. 30-33 There are many available macroinitiators and crosslinkers, and it is also possible to use two different macroinitiators to prepare miktoarm stars. Alternatively, star polymers can be prepared by employing multifunctional core and subsequently growing arms, following core-first approach. The resulting multiarm polymers are effective emulsion stabilizers, even at very low concentrations. 31,34-36 Their adsorbed layers at oil/water (O/ W) interfaces are predominantly elastic in nature. Star polymers with relatively high densities of arms show particlelike behavior at interfaces, and emulsions stabilized by them may be viewed as Pickering systems rather than as more

conventional polymer-stabilized systems. <sup>3,31,36</sup> Pickering stabilized emulsions were first reported by Ramsden and then Pickering <sup>37,38</sup> and have been the subject of much interest in recent times. <sup>1,39–41</sup> In these systems, emulsion droplets are stabilized by particles adsorbed at the oil/water interface rather than conventional surfactants or polymers. Pickering emulsions can show great stability toward coalescence, and it arises from the high adsorption energies of the particles, often of the order of 1000 kT or more, and this leads to irreversible adsorption of the particles at the oil/water interface. <sup>41</sup>

In this paper, the properties of PEO stars based on poly(divinylbenzene) cores with a relatively low density of grafted PEO arms compared to previously reported systems were studied. The viscoelastic nature of these polymers adsorbed at oil—water interfaces was investigated using both interfacial tension and interfacial rheology. The viscoelastic properties of adsorbed layers of polymer, surfactants, or particles at interfaces can be studied using dilatational interfacial rheology in which the interface is subjected to a

Received: March 2, 2023 Revised: May 5, 2023 Published: May 22, 2023





change in area, either oscillatory or as a step change, and the time dependence of interfacial tension is followed. 42-47 In oscillatory dilatational measurements, a sinusoidal change in area causes a variation in the interfacial excess of the adsorbed particles or molecules leading to a sinusoidal change in interfacial tension.<sup>48</sup> Analysis of the variation in interfacial tension with interfacial area and time allows the determination of dilatational interfacial complex modulus,  $\varepsilon^*$ , which is a measure of the overall response of the particle-laden interface to the dilatation. 48,49 As with conventional bulk rheology, the complex modulus can be further broken up into the elastic (storage),  $\varepsilon'$  and viscous (loss),  $\varepsilon''$  components. These are measures of the energy that is either stored elastically or dissipated during the dilation. These parameters allow the nature of the adsorbed layer to be probed in greater detail than by studying interfacial tension alone since the elastic modulus gives information about the variation in interfacial tension with the area of the adsorbed particles. The loss modulus arises from mechanisms that reduce the magnitude of the interfacial tension during the measurement; these include adsorption/ desorption of particles or conformational changes in the adsorbed polymer.45

A number of studies reported in the literature show that adsorbed layers of hydrophobic nanoparticles stabilized by grafted hydrophilic chains, such as star polymers or solid particles with grafted arms, at the oil/water interface are often viscoelastic in nature. 34,36,50,51 This is generally thought to be a contributing factor to emulsion stability where the elasticity of the adsorbed layer may act to reduce or prevent the coalescence of emulsion droplets. 52,53 The elasticity of adsorbed layers particles with grafted hydrophilic arms depends on various parameters, such as the molecular weight, grafting density and composition of the arms,<sup>51</sup> and whether the arms are charged or uncharged, for example, where the arms have pH-dependent groups such as carboxylic acids or amines. 51,54 In general, adsorbed layers of polymers with pHdependent arms show lower interfacial moduli in their charged state than in their uncharged state.<sup>51</sup> In many cases, emulsions stabilized by adsorbed layers showing high interfacial elasticities are often stable toward coalescence. SS-57 However. a high interfacial elasticity alone is not always sufficient to differentiate between good or poor emulsion stabilizers and the exact relationship between emulsion stability and interfacial rheology is not well understood.<sup>47</sup> Lucassen-Reynders<sup>53</sup> suggested that Marangoni effects arising from dilatational elasticity act to reduce the thinning of thin liquid films between droplets, thus preventing coalescence. In essence, thermal fluctuations of an interface cause local expansion of the interface and potential thinning in the film leading to coalescence. The local expansion of the interface that has a measurable interfacial elasticity leads to an increase in interfacial tension. The resulting interfacial tension gradient results in adsorbed molecules or particles being pulled from areas of low tension to the expanding area also dragging the associated bulk phase (water in the case of O/W emulsions) and acts to reduce or prevent the thinning of the film and stabilizing the emulsion. There are several reports in the literature that relate emulsion stability to the dilatational modulus. 47,50,55-57 However, while there is no simple or direct correlation, it is almost certain that a high interfacial modulus will be a significant factor affecting emulsion stability.

Herein, star polymers were synthesized via activators regenerated by electron transfer (ARGET) atom transfer

radical polymerization (ATRP)<sup>58–63</sup> using arm-first technique (Figure 1). Poly(ethylene oxide) (PEO) chains with a molar

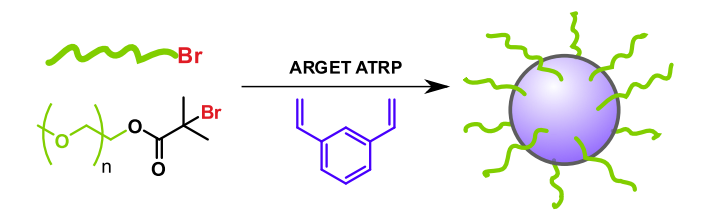


Figure 1. Synthesis of PEO star polymers via the arm-first approach.

mass of either 2 or 5 kDa with terminal  $\alpha$ -bromoisobutyrate ATRP functionalities were used as macroinitiators and divinylbenzene as a crosslinker for arm-first star synthesis.

# EXPERIMENTAL SECTION

**Materials.** Poly(ethylene glycol) methyl ether (PEO<sub>Sk</sub>,  $M_n$  = 5000, Aldrich, and PEO<sub>2k</sub>,  $M_n$  = 2000, Aldrich) was used to prepare poly(ethylene oxide)-based macroinitiators PEO-MI1 and PEO-MI2, following a previously published procedure. DVB, 80%) was purchased from Aldrich and purified by passing through a column filled with basic alumina. Copper dibromide (CuBr<sub>2</sub>, Aldrich, 99%), tin(II) 2-ethylhexanoate (Sn(EH)<sub>2</sub>, 95%, Aldrich), N,N-dimethylformamide (DMF, VWR, 99%), anisole (Acros Organics, 99%), and neutral alumina (standard activity, 50 to 200  $\mu$ m, Sorbent Technologies) were used as received. Tris(2-pyridylmethyl)amine (TPMA) was synthesized according to the previously reported procedure. <sup>64</sup>

**Nuclear Magnetic Resonance Spectroscopy (NMR).** <sup>1</sup>H NMR spectroscopy measurements were performed with a Bruker Advance 500 MHz spectrometer using CDCl<sub>3</sub> as the solvent.

**Gel Permeation Chromatography (GPC).** Number-average MWs  $(M_n)$  and molecular weight distributions of PEO star polymers were determined by GPC. The GPC system used an Agilent Infinity pump and an Agilent Infinity refractive index and light scattering detectors using PSS columns (SDV  $10^2$ ,  $10^3$ , and  $10^5$  Å) with THF as the eluent at a flow rate of 1 mL/min at 35 °C. Toluene was used as the internal standard for the system.

**Synthesis of PEO Stars.** In a typical procedure, PEO macroinitiator PEO-MI1 (1 g, 0.25 mmol) was dissolved in anisole (7.56 mL) in a 10 mL Schlenk flask. To this solution was added a solution of CuBr $_2$  (0.45 mg, 0.002 mmol) and TPMA (5.8 mg, 0.02 mmol) in anisole (0.5 mL). DVB (0.38 mL, 3.75 mmol, 15 molar equivalents vs macroinitiator) was added next, and the flask was purged through four freeze–pump–thaw cycles. Then, a solution of Sn(EH) $_2$  (12.95  $\mu$ L, 0.04 mmol) was added under a nitrogen atmosphere, and the flask was placed in a thermostated oil bath at 90 °C. After 23 h, the reaction was stopped, and the copper catalyst was removed by passing the mixture through a column of neutral alumina. The product was purified by dialysis against methanol for 1 week. PEO stars were characterized by NMR and GPC. The structural features of two prepared star polymers are summarized in Table 1. No unreacted macroinitiator was detected in the final samples.

The 2k and 5k PEO pDVB star polymers were dispersed in reverse osmosis water to form a stock 2% solution and diluted as needed to form solutions at concentrations in the range 0.01-0.2% w/v. Anhydrous n-dodecane (n-C12) and m-xylene were obtained from Sigma-Aldrich and were stored over fumed silica (Aerosil OX-50, Degussa) to remove surface-active impurities and finally filtered through a 0.22 micron PTFE filter. The interfacial tensions of the two oils were determined against reverse osmosis purified water and were found to be close to the literature values (52 and 37 mNm $^{-1}$  respectively).  $^{34,65}$ 

Interfacial Tension and Dynamic Surface Tension. Static droplets of the polymer solutions, typically  $20~\text{mm}^3$ , were formed on a syringe needle of outer diameter 1.65 mm using a 1~mL syringe; the

Table 1. Number of Arms Per Molecule Calculated on the Basis of PEO  $M_n = 2000$  and 5000 Da<sup>aa</sup>

MI	star Mn Da	arms per molecule	core mass fraction	core radius/nm	area per arm/nm <sup>2</sup>
2k PEO	$9.70 \times 10^4$	24.7	0.49	2.6	3.6
5k PEO	$1.16 \times 10^{5}$	16.7	0.28	2.3	4.1

"Core radius estimated from the mass fraction of DVB assuming a bulk density of pDVB of 1.02 g/mL.

droplet was formed in situ within a cuvette containing n-dodecane or m-xylene. The static interfacial tension was determined by videobased profilometry using a DataPhysics ODG20, and measurements were taken at roughly 1 s intervals. The interfacial tension was followed as a function of droplet age using the ODG20 video analysis software, typically for 7200 s or less if the system had reached an equilibrium value within that time. After this equilibration period, the interfacial dilatational viscoelastic properties of the adsorbed layer were determined using the same droplet either by oscillation of droplet volume or by a step change in droplet volume. Repeat measurements showed the error in the interfacial tension to be  $\pm 0.5$  mNm $^{-1}$ .

Dynamic surface tension measurements were made on aqueous solutions of the star polymers using a Kruss BP100 maximum bubble pressure tensiometer at 20  $^{\circ}\text{C}.$  The error in these measurements was known to be  $\pm 0.5~\text{mNm}^{-1}.$ 

Oscillation Interfacial Rheology. The volume of the equilibrated droplets described above was then varied sinusoidally using a piezo-electric actuator for five complete oscillations giving 200 images. This was carried out at 0.01, 0.02, 0.05, 0.1, 0.2, 0.5, and 1 Hz at an amplitude that produced a fractional interfacial area variation of 5–10%, this corresponded to a 0.1–0.15 mm amplitude of the actuator. The sequences of images of the drop oscillations were analyzed to give plots of interfacial tension and droplet area as a function of time. Fourier transform of the interfacial tension vs time data extracted the interfacial moduli ( $\varepsilon'$  and  $\varepsilon''$ ) at each frequency. On selected samples, additional amplitude sweeps were carried out in which the fractional area change was varied between ca. 1 and 15% at a constant frequency of 0.1 Hz, in all other respects the method was the same as described above.

The interfacial area (A(t)) of the droplets was varied sinusoidally with an amplitude of  $\Delta A$  about its mean value,  $A_o$ , with time such that

$$A(t) = A_0 + \Delta A \cos(\omega t) \tag{1}$$

Each image was analyzed using the instrument software to give the variation in interfacial tension with  $(\gamma(t))$ . The amplitude of the interfacial oscillation was determined  $(\Delta \gamma)$  and the variation of the interfacial tension during the oscillation is given by <sup>66</sup>

$$\gamma(t) = \gamma_o + \Delta \gamma \cos(\omega t + \phi) \tag{2}$$

where  $\phi$  is the phase angle between the sinusoidal variations in area and interfacial tension. The instrument software applies a Fourier transform to the variation in interfacial tension and area to extract  $\varepsilon'(\omega)$  and  $\varepsilon''(\omega)$  at each individual frequency, where

$$\varepsilon'(\omega) = \Delta \gamma(\omega) \frac{A_o}{\Delta A} \cos \phi(\omega)$$
 (3)

and

$$\varepsilon''(\omega) = \Delta \gamma(\omega) \frac{A_o}{\Delta A} \sin \phi(\omega)$$
 (4)

In general, three repeat runs were carried out on each solution/oil phase combination, including fresh solutions and oil phases and also repeat runs on the same droplet. The repeatibility was assessed by determining the averages and standard deviations of the moduli obtained at each frequency for all spectra obtained on each sample. The standard deviation was found to vary little between samples and frequencies and the mean value of all values was taken as the experimental error. The mean standard deviation obtained for the elastic moduli was of the order of  $\pm 0.8~\rm mNm^{-1}$ , while  $\pm 0.2~\rm mNm^{-1}$  was obtained for the loss modulus. For repeat runs on the same

droplet, the average magnitudes showed ranges of  $\pm 0.2$  and  $\pm 0.1$  mNm<sup>-1</sup> for  $\varepsilon'$  and  $\varepsilon''$ , respectively. Representative plots for each sample are shown here, and typical sets of repeat spectra are shown in the Supporting Data.

**Interfacial Relaxation.** The frequency response of the adsorbed interfacial layer was further probed using interfacial relaxation, in which the return to equilibrium interfacial tension after a step change in interfacial area was determined. Droplets were formed in the same manner as described above for the interfacial tension determination and the volume of the equilibrated droplet was then rapidly increased using the piezo-electric actuator of the ODG 20, typically a 0.1-0.15 mm displacement of the actuator was used on the timescale of 0.1-0.2 s. The increase in area resulted in an increase in interfacial tension that then decayed back to the equilibrium value. The interfacial tension was determined by image analysis of a video recording of the droplet shape before and after the area increase for 1000–1200 s. The frame rate of the video was set to 25 fps at the point of increase but was then reduced exponentially over time to around 1 fps after 1000 s; this was to ensure sufficient data points in the short-time region of the interfacial tension decay but to limit the number of images requiring image analysis.

The interfacial dilatational response of the adsorbed layers was determined using Fourier transform analysis of the interfacial tension decay  $(\Delta \gamma(t))$  after the sudden expansion  $(\Delta A)$ . The sudden expansion of an equilibrated interface reduces the interfacial excess of the adsorbed material leading to an increase in interfacial tension, which then decays over time as the adsorbed layer returns to equilibrium (Figure 2).

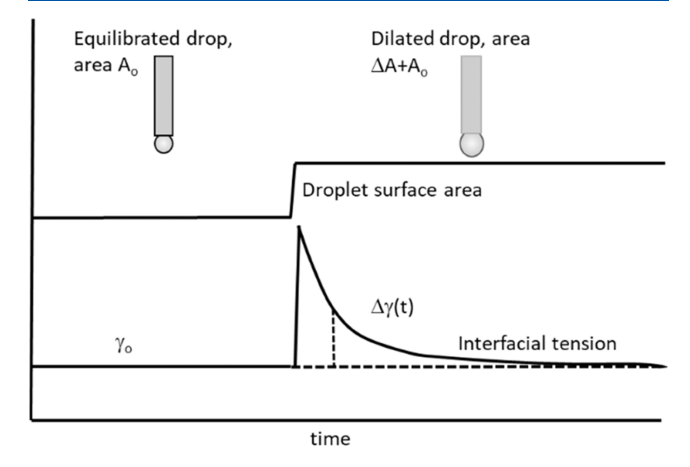
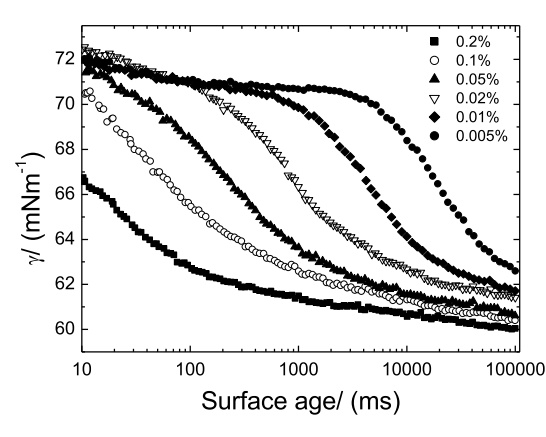


**Figure 2.** Decay of interfacial tension after a sudden expansion of an interface.

Fourier transformation (FT $\Delta\gamma(t)$ ) of the interfacial tension decay,  $\Delta\gamma(t)$ , back to the equilibrium value allows the frequency dependence of the interfacial moduli ( $\varepsilon^*(\omega)$ ,  $\varepsilon'(\omega)$ , and  $\varepsilon''(\omega)$ ). The Fourier transform for this process is given by  $^{46,67-70}$ 

$$\varepsilon^*(\omega) = \frac{\text{FT}(\Delta \gamma(t))}{\text{FT}\left(\frac{\Delta A(t)}{A_o}\right)} = \frac{\int_0^\infty \Delta \gamma(t) e^{-i\omega t} dt}{\int_0^\infty \left[\frac{\Delta A(t)}{A_o}\right]} e^{-i\omega t} dt$$
(5)

Since the timescale of the change in interfacial area is relatively short compared to the decay rate, it can be approximated as a Heaviside step function,  $\Delta A(t)/A_{\rm o}=0$   $t\leq 0$  and  $\Delta A(t)/A_{\rm o}=\Delta A/A_{\rm o}$  t>0, for which



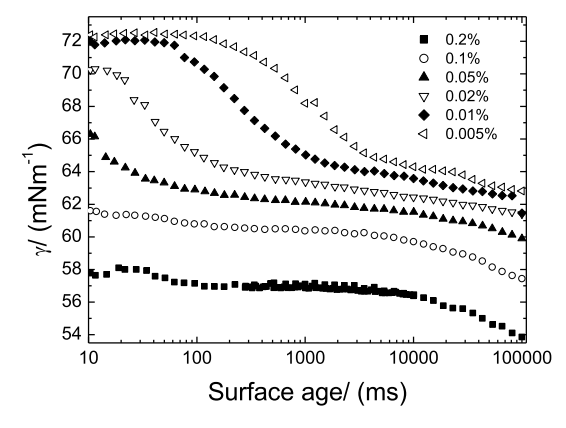


Figure 3. Short-time dynamic surface tension of 2k PEO (left) and 5k PEO (right) homo-arm star polymers (error in the dynamic surface was  $\pm 0.5$  mNm<sup>-1</sup>).

$$\int_0^\infty \frac{\Delta A(t)}{A_o} e^{-i\omega t} dt = \frac{\Delta A}{i\omega A_o}$$
 (6)

It is convenient to define the decay function  $\beta(t)$ , where

$$\beta(t) = \frac{A_{o}\Delta\gamma(t)}{\Delta A} \tag{7}$$

The complex interfacial modulus  $\varepsilon^*(\omega) = \varepsilon'(\omega) + i\varepsilon''(\omega)$  and so the Fourier transform may be split into its real and imaginary components

$$\varepsilon'(\omega) = \beta(\infty) + \omega \int_0^\infty (\beta(t) - \beta(\infty)) \sin(\omega t) dt$$
 (8)

and

$$\varepsilon''(\omega) = \omega \int_0^\infty (\beta(t) - \beta(\infty)) \cos(\omega t) dt$$
(9)

where  $\beta(\infty)$  relates to the value of the decay function at infinite time in the case of where the system does not fully relax back to the initial value, in this work the system fully recovered back to equilibrium giving  $\beta(\infty) = 0$ 

The integrals of Fourier transforms eqs 8 and 9 were numerically evaluated within Excel in the frequency range 0.0001–1 rad s<sup>-1</sup>. The Fourier transform requires evenly spaced time points and so the whole of the decay function was fitted to a double or triple exponential decay to accurately reproduce the data at 0.2 s intervals using the nonlinear double and triple exponential fitting routines in Origin v.6 (MicroCal).<sup>67–70</sup>

$$\beta(t) = \beta(\infty) + \sum_{i=1}^{n} A_i e^{-t/k_i}$$
(10)

where n = 2 or 3.

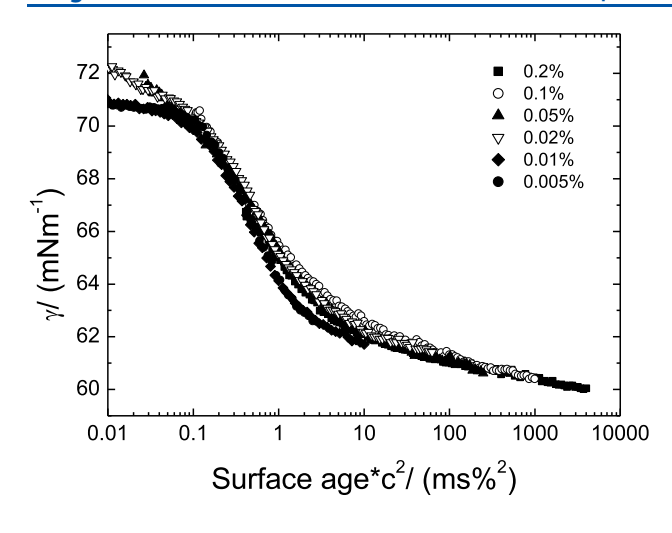
The error in the moduli obtained from the relaxation measurements was assessed as being of the order of  $\pm 10\%$  based on two repeated measurements.

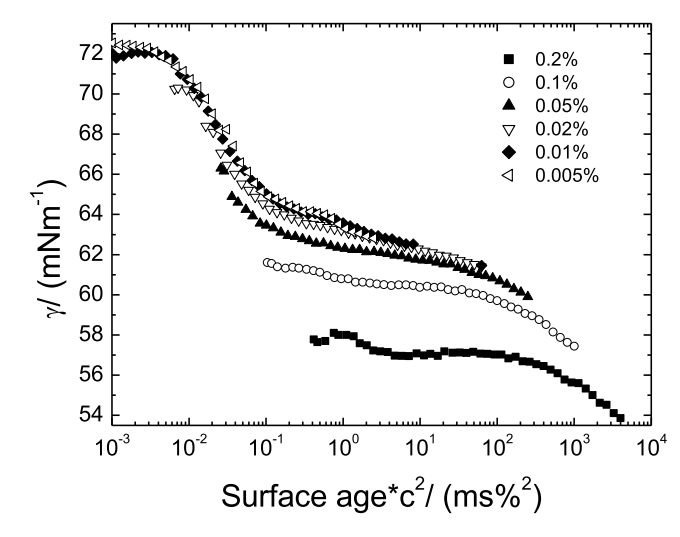
**Emulsion Stability.** 10% v/v oil-in-water emulsions were prepared by premixing 1 mL of *n*-dodecane in 9 mL of 0.2% polymer solutions and shaken by hand to give coarse droplets. These were further emulsified by subjecting the system to ultrasonic agitation for 30 s using an ultrasonic probe with a 3 mm tip. The samples were stored at 20 °C and periodically sized using a Malvern 2000 laser diffraction system, three measurements being made at each time point. The effect of the concentration of 5k PEO on *n*-dodecane in water emulsions was also investigated by repeating the above method but with a range of 5k PEO concentrations (0.01–0.2% w/w).

# RESULTS AND DISCUSSION

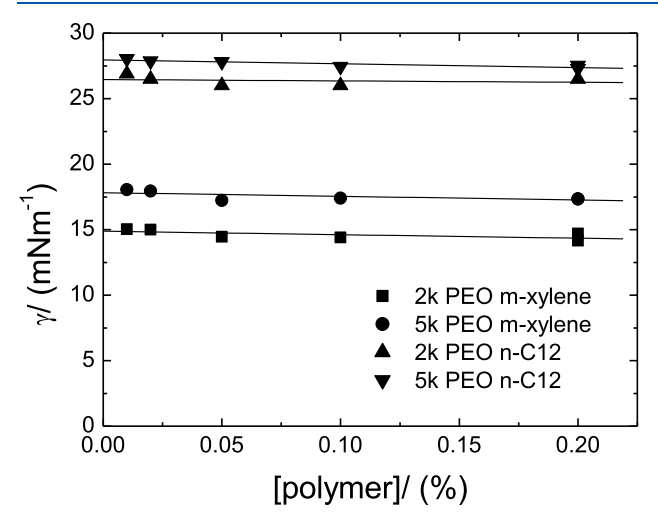
Both 2k and 5k PEO star polymers reduced the surface tension of water although by a relatively small amount compared to typical surfactants. The 2k PEO sample tended to the same long-time surface tension (100 s) of around 60 mNm<sup>-1</sup>, and the results showed the same general behavior as surfactant solutions above their critical micelle concentration. The rate of decrease in surface tension increased with increasing concentration due to the increased rate of diffusion to the surface at higher concentrations. While the 2k PEO tended to a long-time surface tension of around 60 mNm<sup>-1</sup> at all concentrations, the situation was less well defined with the 5k PEO sample. This polymer did not tend to a single value of the surface tension at longer times for all concentrations. For concentrations up to and including 0.05%, the solutions appeared to be approaching plateau values in the range of 62-64 mNm<sup>-1</sup> around a surface age of 1000 ms; however, the data then appear to begin to fall once more at larger surface ages. This was much more pronounced at 0.1 and 0.2% of the 5k PEO star polymer; at these concentrations, the dynamic surface tension varied little at somewhat lower values of 61 and 57 mNm<sup>-1</sup>, respectively, between 10 and about 100 ms. However, at longer times, both samples showed a significant drop in dynamic surface tensions. The reason for this is not known but may represent the reorientation of the longer poly (ethylene oxide) chains of the 5k sample surface to a more favorable conformation. The 2k samples with their shorter arms and 50% greater grafting density would be expected to show less freedom compared to the higher-molecular-weight poly(ethylene oxide) chains in the 5k sample where the outer segments of the chains would have some degree of freedom to reorientate over a longer time to reduce their interfacial energy.

The concentration and time dependence of the dynamic surface tension of surfactants has been considered by Ferri et al. 70 who found that the kinetics can be understood in terms of the timescale of diffusion to the interface. The same treatment will be used here for the particles rather than surfactant molecules. If the adsorption of the particles, at a concentration c, is governed by simple diffusion (effective diffusion coefficient (D)) and the surface excess ( $\Gamma$ ) is independent of concentration (ie. plateau adsorption), then the timescale of the adsorption and reduction of surface tension is related to characteristic adsorption time  $\tau_D = \Gamma^2/Dc^2$ . Ferri<sup>70</sup> found that the characteristic adsorption time depends on the extent of the "adsorption" depth,  $\delta$ . This is the distance into the bulk that would be completely depleted by the equilibrium surface excess. The amount adsorbed over an area dA is dA $\Gamma$ . This would then correspond to a volume  $c\delta dA$  of the bulk solution containing an equal amount of adsorbate and  $\delta = \Gamma/c$ . The time required for material to diffuse a distance  $\delta$  is  $\delta^2/D$ 





**Figure 4.** Dynamic surface tensions of 2k (left) and 5k PEO (right) star polymers at the air—water interface plotted against the normalized timescale of  $t_{\text{surf}}/c^2$  (error in the dynamic surface tension,  $\pm 0.5 \text{ mNm}^{-1}$ ).



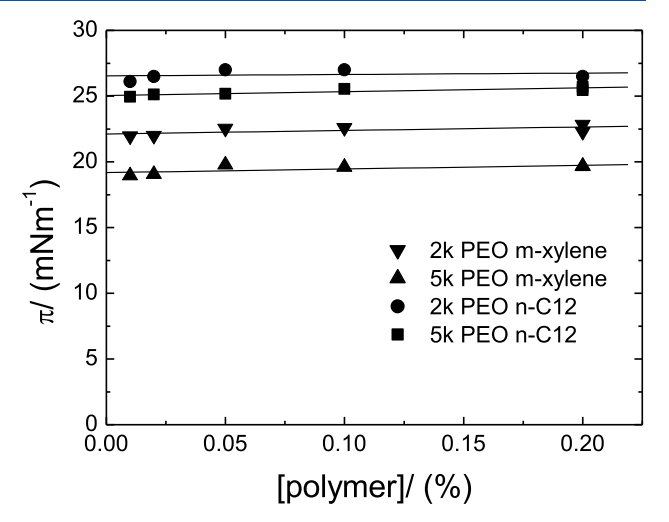


Figure 5. Variation in interfacial tension (left) and interfacial pressure (right) with star polymer concentration (error in the interfacial tension and pressure was  $\pm 0.5 \text{ mNm}^{-1}$ ).

leading to the equation above for the characteristic diffusion time. If the process falls under these conditions, then the dynamic surface tension plots should collapse onto a single master curve when the surface age  $(t_{\rm surf})$  is normalized to reduced time as  $t_{\rm surf}/\tau_{\rm D}$ , or more simply  $t_{\rm surf}c^2$ .

The applicability of this approach can be seen in the collapse of the dynamic surface tension curves obtained for the 2k PEO star polymer at the air/water surface. The DST for this polymer (Figure 3) tended to the same long-time value for all concentrations studied, and the effect of changing the concentration was simply to move the curve to higher or lower surface ages. Figure 4 shows the data with the surface age normalized by multiplying by  $c^2$ . Since the dynamic surface tension tended to essentially the same value for all concentrations, then the surface excess would be independent of concentration. Any variation in diffusion coefficient with concentration would be negligible then if the adsorption of the star polymers is diffusion-controlled, then the data should collapse on the reduced timescale of  $t_{\text{surf}} c^2$ . The data for the 2k PEO star collapsed extremely well onto a single curve showing that the process was well described by the simple diffusion/ adsorption model of Ferri. A similar plot for the 5k PEO star

polymer was not as tightly collapsed as for the 2k variant; this was likely due to a small variation in equilibrium surface tension and surface excess with concentration. However, the collapse of the data at the lower concentrations, although not perfect, still suggested that the process was predominantly controlled by particle diffusion to the interface.

The equilibrium interfacial tensions between the two polymers and *n*-dodecane or *m*-xylene are shown as a function of concentration in Figure 5. In all four cases, the interfacial tension showed little variation with concentration. The interfacial tension was mostly governed by the oil phase with the higher values seen with *n*-dodecane (26–28 mNm<sup>-1</sup>) compared to those with *m*-xylene in the range 15–17 mNm<sup>-1</sup>. The molecular mass of the polymer had a small but consistent effect with both oils with the 2k PEO showing lower values than the 5k PEO, the difference being ca. 3 mNm<sup>-1</sup> with *m*-xylene and 1 mNm<sup>-1</sup> with *n*-dodecane.

The interfacial pressure,  $\pi$  (=  $\gamma$  -  $\gamma_o$ , where  $\gamma_o$  is the interfacial tension of the clean interface) also depended on the oil phase with those for the 5k PEO star at the *n*-dodecane/water interface being of the order of 6 mNm<sup>-1</sup> higher than at the *m*-xylene/water interface, while the difference was 4

mNm<sup>-1</sup> with the 2k PEO star. Higher interfacial pressures have previously been reported for 2k PEO stars (64 arms) at the cyclohexane/water interface compared to the m-xylene/water interface.<sup>34</sup> This was attributed to the PEO chains being more constrained at the cyclohexane/water interface than at the mxylene/water interface. The aliphatic hydrocarbon is a poor solvent for PEO that disfavors any penetration of the arms into the oil phase and any arms that enter the phase will likely be in a collapsed conformation, whereas the aromatic m-xylene is a much better solvent for the PEO chains resulting in greater penetration and well solvated and expanded conformation. According to Huang et al., the resulting differences in interfacial tension are due to enthalpic contributions from segment/solvent interactions and entropic factors arising from the differences in the conformation of the arms on the adsorbed particles in the different solvents.3

The differences between the 2k and 5k PEO variants are also shown by the time dependence of the approach of the interfacial tension toward equilibrium. Interfacial tension versus time plots are shown for 0.1% polymer for all four polymer/oil phase combinations in Figure 6. It is apparent that

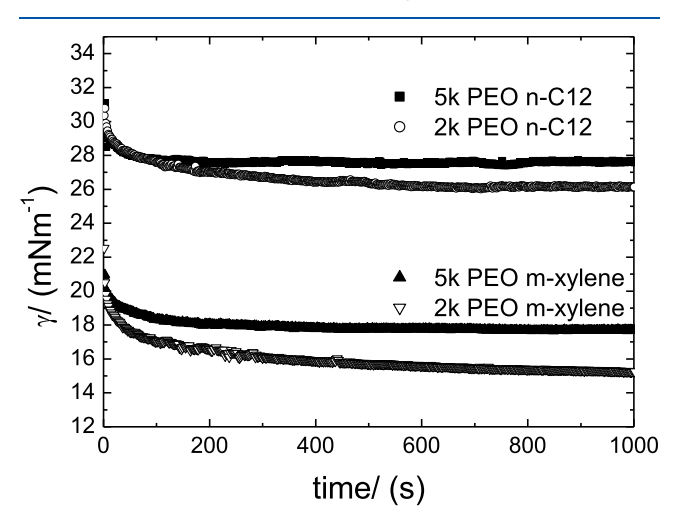


**Figure 6.** Interfacial tension vs time plots for the four polymer/oil phase (n-dodecane or m-xylene) combinations at an aqueous polymer concentration of 0.1% (error in the interfacial tension was  $\pm 0.5$  mNm<sup>-1</sup>).

the 5k PEO equilibrates more rapidly than the 2k PEO with both oils; this is more clearly demonstrated by plotting the reduced interfacial tension as a function of time.

The reduced interfacial tension,  $\gamma_{\rm red}$  is given by  $^{50}$ 

$$\gamma_{\rm red} = \frac{\gamma(t) - \gamma_{\rm eqm}}{\gamma_{\rm o} - \gamma_{\rm eqm}} \tag{11}$$

where  $\gamma(t)$  is the interfacial tension at time t, and  $\gamma_{\rm o}$  and  $\gamma_{\rm eqm}$  are the oil/water and equilibrium interfacial tensions, respectively. Plots of the reduced surface tension versus time are shown in Figure 7 for all four polymer/oil combinations.

Despite their similar total molecular masses, it is clear from the reduced interfacial tension plots that at both the *m*-xylene and *n*-dodecane water interfaces, the 5k PEO star reaches the equilibrium tension (when the reduced interfacial tension reaches zero) around 10 times quicker than the 2k PEO variant. This suggests that the more hydrophilic and water-soluble 5k PEO star tends to sit on the interface with its core

penetrating to a lesser extent into the oil phase than the more hydrophobic 2k PEO star.

Comparison of the adsorption rates of the 5k PEO star at the m-xylene and n-dodecane interfaces shows that equilibrium is reached more rapidly at the n-dodecane interface. The hydrophobic pDVB core needs to be in contact with and wetted by the oil phase for the polymer to adsorb strongly at the interface. The PEO arms show a greater solubility m-xylene<sup>34</sup> and so will readily penetrate into the aromatic oil, whereas they show a much lower solubility in the aliphatic n-dodecane and will not so tend to readily penetrate. Thus, the hydrophobic core will be pulled through the interface and further into the oil phase by penetration of the PEO into the m-xylene allowing good wetting of the core. At the water/n-dodecane interface, the lower and less favorable penetration results in the core penetrating to a lesser extent resulting in the polymer sitting more on the interface.

Surprisingly, the 2k PEO star polymer show virtually identical kinetics of adsorption at both the *n*-dodecane/water and the *m*-xylene/water interfaces. This suggests that the interaction of the 2k PEO chain with the aqueous or either of the two oil phases is less important than the wetting of the core itself by either oil. At the higher-arm molecular weight of 5k, the PEO interactions make a greater contribution to the adsorption of the star polymers, leading to the absolute value of the interfacial tension of the 5k PEO star polymers being systematically higher than the shorter-chain analogue at both oil/water interfaces studied.

Reports in the literature have found that star polymers of pDVB cores stabilized by 64 arms of 2000 g/mol PEO adsorbed at oil/water interfaces to produce an interfacial layer that is predominantly elastic in nature.<sup>34</sup> Additionally, at the concentrations studied (0.0005-0.1%), the elastic modulus was essentially independent of frequency and increased with increasing concentration. The results obtained here with star polymers with lower grafted arm density show somewhat different behavior. At 0.01%, all four systems showed frequency-independent behavior, the magnitude of the moduli being primarily determined by the polymer ethylene oxide molecular mass. At both the n-dodecane and the m-xylene/ water interface, the 2k PEO star polymer gave elastic moduli in the range of 14-15 mNm<sup>-1</sup> at the higher frequencies (Figure 8), compared to the lower values of 5-7 mNm<sup>-1</sup> seen with the 5k PEO star at either of the two interfaces. However, the responses became more frequency-dependent as the concentration increased for all four pairings of polymer and oil phase. The responses were predominantly elastic with  $\varepsilon' > \varepsilon''$ , with  $\varepsilon''$ decreasing with increasing frequency and decreasing concentration. This can be summarized in plots of the phase angle,  $\phi$ , where tan  $\phi = \varepsilon''/\varepsilon'$ , against frequency for the various concentrations, Figure 9. The phase angle decreased with increasing frequency and decreasing concentration as the interfaces became increasingly dominated by the elastic response. All four of the polymer/oil phase pairings showed similar behavior to that shown in Figure 8 and Figure 9.

In most cases, it was observed that the elastic modulus at 1 Hz was generally lower than that at 0.5 Hz. Initially, it was assumed that this was due to a coupling of the interfacial rheological properties and the viscosities of the aqueous and oil phases. Freer et al.<sup>71</sup> have shown that a viscosity difference between the two phases can lead to progressively nonsinusoidal response of the interfacial tension to a sinusoidal oscillation in droplet area. The importance of this can be

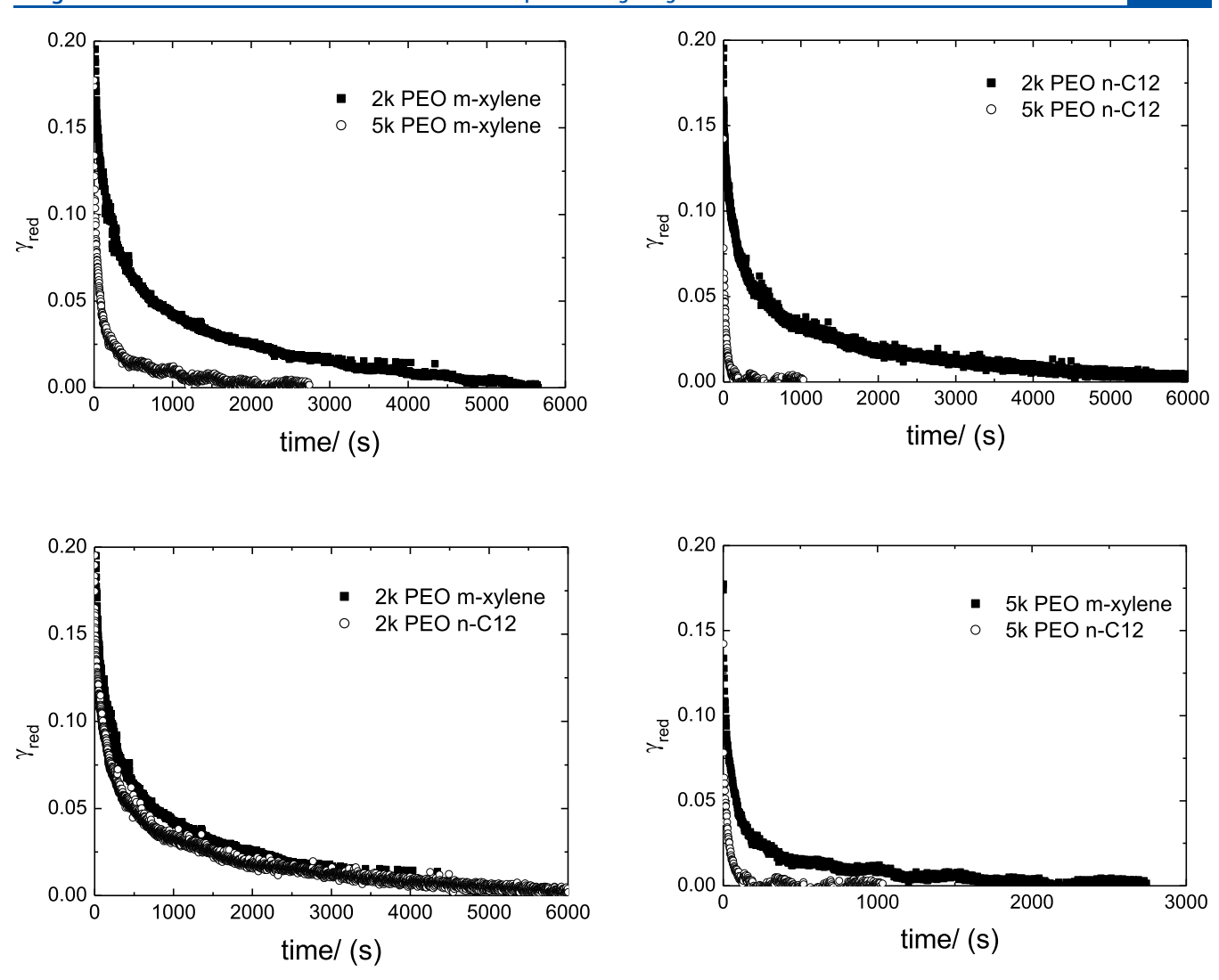
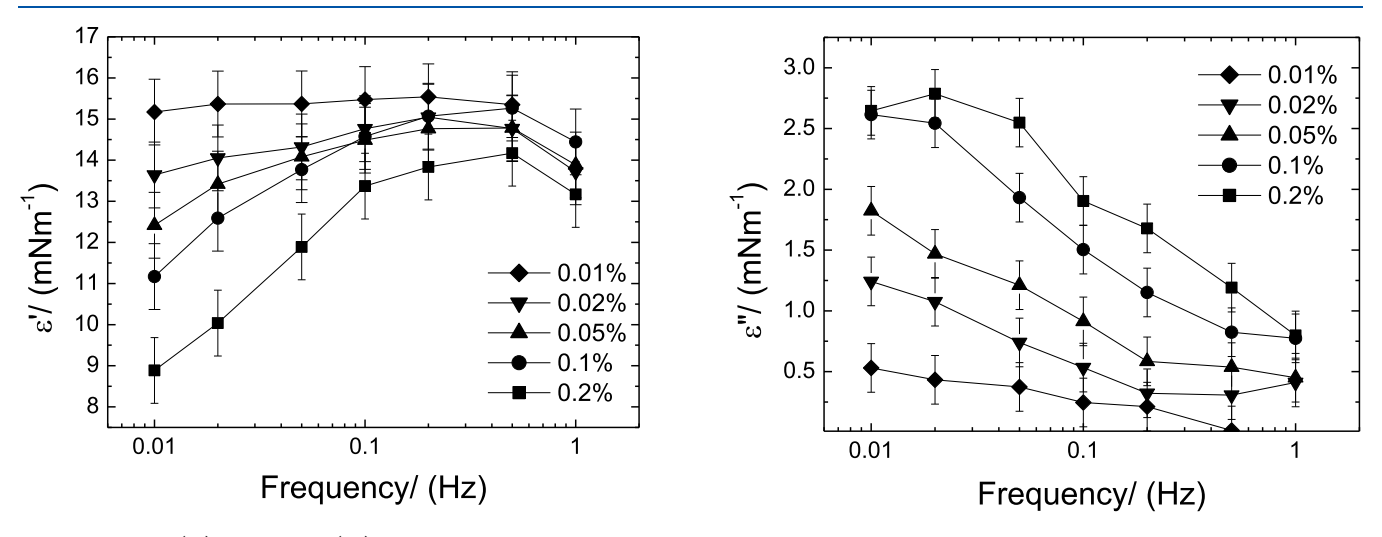


Figure 7. Reduced interfacial vs time plots for the four polymer/oil phase (n-dodecane or m-xylene) combinations at an aqueous polymer concentration of 0.1%.



**Figure 8.** Elastic ( $\varepsilon'$ ) and viscous ( $\varepsilon''$ ) interfacial moduli as a function of frequency for 2k PEO star nanoparticles adsorbed at the *m*-xylene/water interface for various aqueous concentrations.

$$C_{\rm a} = \Delta\mu\omega\Delta\nu/\gamma R_{\rm c}^{2} \tag{12}$$

estimated from the magnitude of the capillary number,  $C_{\rm a}$ , for the oscillatory motion.

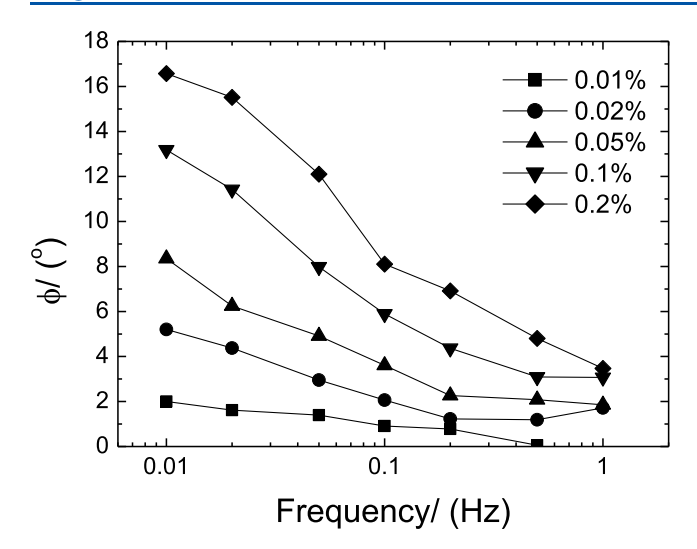


**Figure 9.** Phase angle,  $\phi$ , as a function of frequency for 2k PEO star nanoparticles adsorbed at the m-xylene/water interface at various aqueous polymer concentrations.

where  $\Delta \mu$  is the viscosity difference between the two phases (eg.  $3.44 \times 10^{-4}$  Pas for *n*-dodecane/water),  $\omega$  is the frequency of oscillation (6.28 rads<sup>-1</sup>),  $\Delta \nu$  is the amplitude of the volume oscillation (typically  $2 \times 10^{-9}$  m<sup>3</sup>), and  $R_c$  is the capillary diameter (0.825  $\times$  10<sup>-3</sup> m). This yields representative  $C_a$ values of  $2.5-4.5 \times 10^{-4}$  for the *n*-dodecane systems. Freer et al. suggest that viscous coupling should be negligible for capillary numbers less than  $2 \times 10^{-3}$ . Since the present system was within an order of magnitude, it is possible that the small decrease seen (typically 10%) may be a result of the onset of this effect. However, while some deviation from sinusoidal behavior was seen in the interfacial tension during the oscillation in some cases, it was not readily apparent in all systems where this decrease in modulus was seen. Again, this may suggest that the systems were close to the onset of this effect and the deviation from sinusoidal behavior was present but not obvious. It also possible that the decrease is due to instrumental artifacts resulting from the frame rate of the video camera (25 fps) and the timescale of oscillation. It should be noted that Alvarez et al.<sup>50</sup> also reported a similar drop in elastic modulus for similar star particles at the m-xylene or cyclohexane/water interfaces. In their experimental setup, the

capillary number was of the order of  $1 \times 10^{-6}~\omega$ , which represents an order of magnitude lower than seen here and less likely to show any viscous coupling. This may suggest that the effect is real but unaccounted for theoretically. As a result, the data at 1 Hz should be viewed with caution owing to the uncertainty in the accuracy at this frequency.

It has also been reported that stars with 460 arm 2k PEO stars and 4.5 nm pDVB cores showed a nonsinusoidal behavior where some truncation in the interfacial tension response to a sinusoidal area change was seen at a 1% area change and a frequency of 3 Hz.36 All of the samples studied here showed good sinusoidal behavior with no obvious truncation of the data, Figure 10 shows a typical dataset for 0.1% 2k PEO at the *n*-dodecane/water interface. The cause of truncation was thought to be due to the compression of the adsorbed layer of particles and their subsequent ejection from the interface. The absence of this effect may be a reflection of the softer nature of the interactions between the current particles with 24.7 arms adsorbed at an area of 4.1 nm<sup>2</sup> per arm at an interface compared to the harder interactions between the more particulate-like star polymers with 460 arms at 0.54 nm<sup>2</sup> per arm.<sup>36</sup> The higher-chain-density molecules show a more particulate manner due to a lower conformational freedom of the PEO arms compared to the lower-arm-density molecules acting more akin to adsorbed polymers with a hydrophobic with greater freedom.

Huang et al. studied the interfacial dilatational elasticity of similar star polymer particles consisting of pDVB cores stabilized by 64 2k PEO arms at the cyclohexane/water and m-xylene/water interfaces.<sup>34</sup> The adsorption depended on whether the polymer was dispersed in the water or in the organic phase. Interfacial moduli obtained with polymer dispersed in the aqueous phase varied between ca. 10 and 13 mNm<sup>-1</sup> in the concentration range 0.01–1% at both interfaces, which is in surprisingly good agreement with that found here with the 2k PEO star polymers considering the lower number of arms per molecules (24.7). Other than the reduction in the elastic modulus at higher frequencies (approaching 1 Hz), their system showed little variation in modulus down to  $5 \times 10^{-3}$  Hz in the concentration studied (0.001-0.1%). The latter is in some contrast to that found here in that the 0.1% 2k or 5k PEO star polymers showed a definite frequency dependence, even allowing for any difference in particle size. The reason for

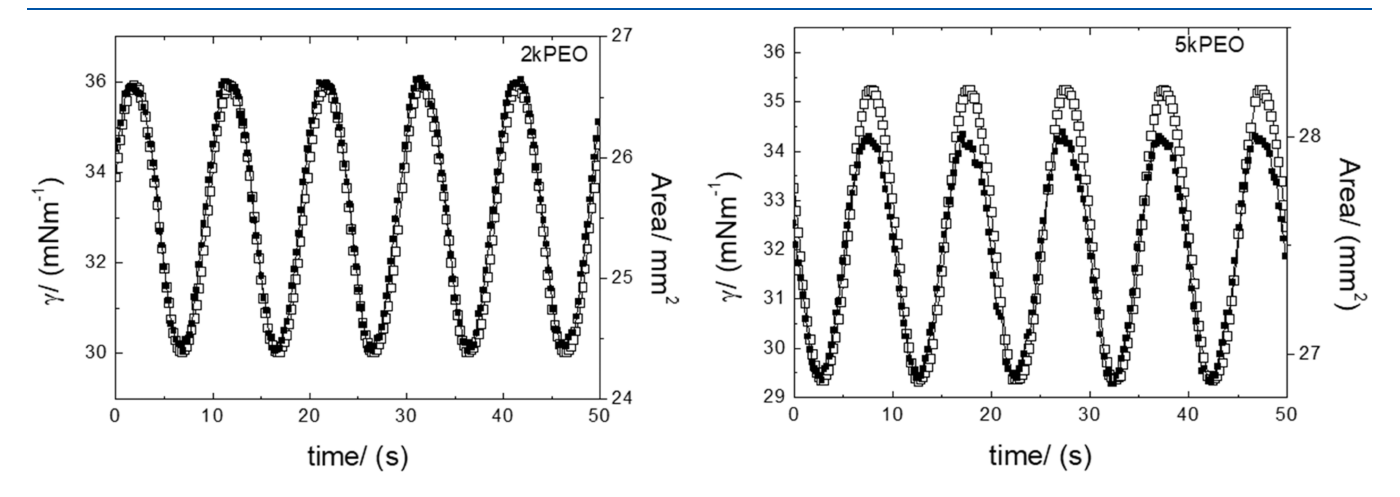


Figure 10. Variation in interfacial tension and droplet interfacial area with time for adsorbed layers of 2k PEO (left) and 5k PEO (right) at the n-dodecane/0.1% polymer aqueous solutions interface.

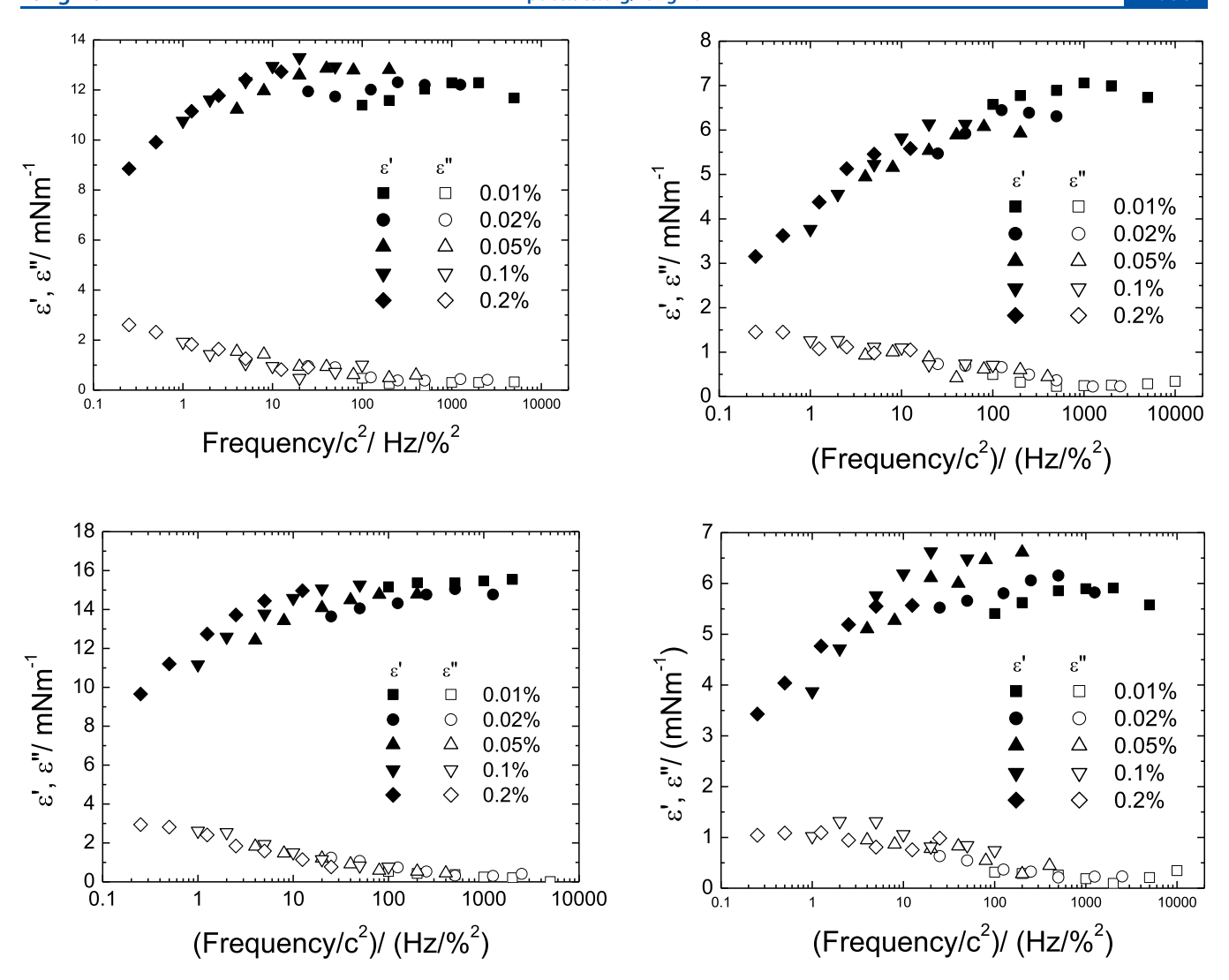
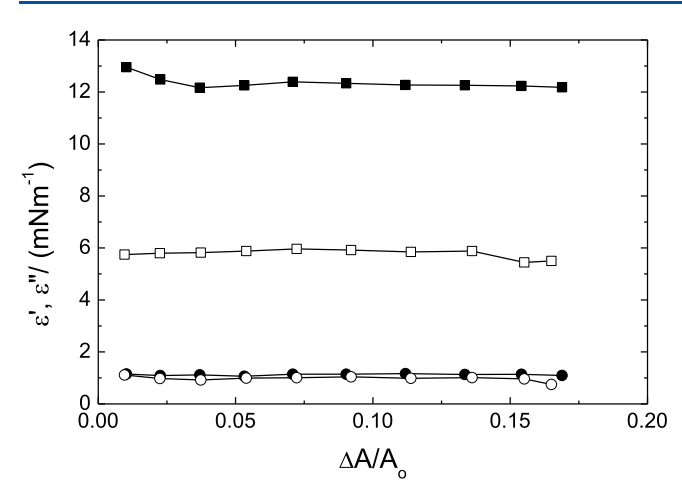


Figure 11. Plots of  $\varepsilon'$  and  $\varepsilon''$  vs reduced frequency for 2k (right) and 5k PEO (left) stars at the *n*-dodecane/water (top) and *m*-xylene/water (bottom) interfaces.

the difference is not clear but may be due to the difference in the number of arms per particle (64 compared to 16.7-24.7 arms per molecule in the present work). The lack of frequency dependence was attributed to the strength of adsorption of the polymers preventing any adsorption/desorption of the particles to and from the interface during oscillation.<sup>34</sup> The likely greater particulate nature of the higher-arm-density polymers would also lead to a higher adsorption energy. This would result in a highly elastic interface with the interfacial tension decreasing and increasing as the interfacial area increased and decreased, respectively. Transport to and from the interface during oscillation would introduce a time- and concentration-dependent relaxation process that would result in a frequency-dependent modulus. It is clear from Figure 8, that for the 2k PEO star at the m-xylene/water interface, the frequency dependence increased with increasing polymer concentration, suggesting that there is a concentrationdependent adsorption/desorption process, which was seen with all four polymer/oil phase pairings. This is also demonstrated by plots of the phase angle,  $\phi$ , vs frequency for the different polymer concentrations of 2k PEO vs mxylene (Figure 9). Again, in all four cases, the phase angle increased with increasing concentration over the entire

frequency range. As mentioned above, it is thought that the star polymers with a low grafted PEO density will act as intermediates between particles and simple polymers adsorbed at the interface. While the hydrophobic core confers some particulate behavior, the majority of the polymer is composed of a relatively diffuse layer of PEO.

The frequency dependence seen in the present systems suggests that there is a significant relaxation process occurring at the interface on the timescale of the oscillation that was not seen with 64 arm 2k PEO particles.<sup>34</sup> In a similar vein to the normalization of the dynamic surface tension data, it is common in bulk rheological studies to normalize the frequency by multiplying it by the relaxation time to give a dimensionless frequency. Despite this approach working well with the dynamic surface tension, it was not expected to apply to the interfacial rheology. Assuming that the relaxation time was related to Ferri's characteristic adsorption time<sup>70</sup> for diffusioncontrolled dynamic surface tension, the frequency response of each system was normalized to the reduced frequency by multiplying the frequency by the relaxation time such that the frequency was divided by  $c^2$  (as opposed to multiplied in the case of the surface age in the DST).



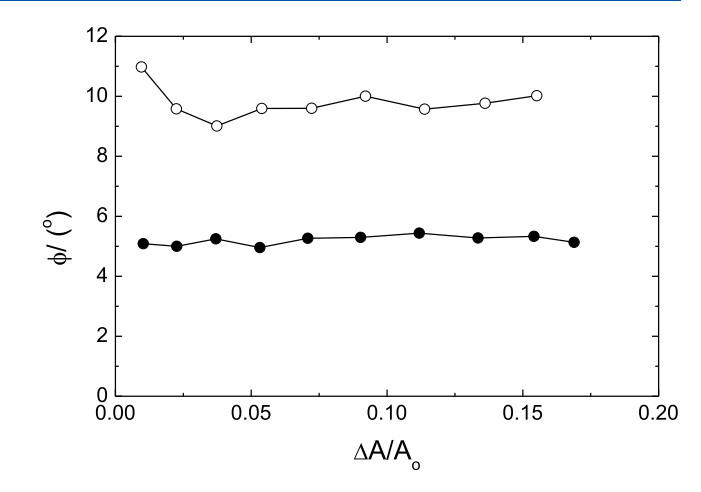


Figure 12. Fractional area amplitude sweeps at 0.1 Hz for 2k PEO (solid symbols) and 5k PEO (open symbols) polymers adsorbed from 0.1% solutions at the n-dodecane/water interface, with (left) elastic (■, □) and loss moduli (●, ○) plotted as a function of fractional area amplitude, and (right) phase angle plotted against fractional area amplitude.

Figure 11 shows the oscillation data for the 5k and 2k PEO star polymers at the n-dodecane/water and m-xylene/water interfaces plotted against the reduced frequency. While not a perfect collapse, the data does reduce to close to a single master curve for each system. The collapse of the oscillation data onto almost a single curve shows that the equilibrium composition of the interface is essentially independent of concentration, as suggested by the concentration-independent equilibrium tension. The differences in frequency response seen at different concentrations are due to differences in the rate of desorption/adsorption during the oscillation. In pure particle-stabilized Pickering emulsions, the adsorption energy of the particles is typically of the order of  $10^4-10^5$  kT, <sup>40</sup> and is normally thought of as being irreversibly adsorbed. Under these conditions, there would be no adsorption /desorption during the oscillation leading to frequency-independent responses. The star polymers used here appear not to be purely particulate in nature but intermediate between a particle and a polymer. For instance, the high adsorption energy of particles arises from the loss of energetically unfavorable oil/ water interface and its replacement with more favorable oil/ particle and particle/water interfaces. This effect is not clear cut in the case of star polymers, for although there is a hydrophobic core acting as a particle, the majority of the adsorbed polymer is composed of PEO arms. Consequently, the behavior of adsorbed polymers is likely to show intermediate behavior between pure polymers and particles with a lower adsorption energy, which allows some adsorption and desorption

The data obtained here show differences to that reported by Huang for similar systems,<sup>34</sup> where they saw less frequency dependence compared to the current systems at comparable concentrations. Although this is attributed to the difference in grafting density of PEO chains on the particles, it should be noted that the measurements reported by Huang et al.<sup>34</sup> were carried out at a lower fractional area amplitude of 3% compared to the 5–10% used here. A possible reason for the increased frequency dependence may then have been a result of the larger dilation of the surface allowing the adsorbed particles greater surface mobility and ease of adsorption and desorption. To determine whether this was the case, the moduli of 0.1% dispersions of the 2k and 5k PEO star samples at the n-dodecane/water were determined at a constant

frequency of 0.1 Hz as a function of applied dilation, in the range of 1–14%. The data are plotted in Figure 12, and it is clear that the moduli were essentially independent of the area change. A small difference was seen at the lowest amplitude (ca. 1%), but this was due to experimental error arising from the very small variation in interfacial tension at this area change (ca. +/- 0.05 mNm<sup>-1</sup>) being of comparable size to the error in the determination of the tension. The phase angle,  $\phi$ , is a sensitive measure of changes in the adsorption and desorption, but this was also independent of area change (Figure 12). From these data, it was concluded that the enhanced frequency dependence was not due to the difference in the fractional area in the two studies.

Determination of the interfacial moduli using oscillation is limited at low frequencies since each individual frequency requires at least one full oscillation (preferably 5 full cycles) and as such the time required increases with the reciprocal of the decreasing frequency. In a relaxation measurement, essentially all frequencies are studied in one run and the measurement time depends on the rate of decay of the sample back to equilibrium or the lowest frequency required to be studied. Thus, interfacial relaxation allows the low-frequency processes to be studied, although care must be taken to ensure equilibrium has been reached prior to the relaxation to ensure accurate values for the decay function,  $\beta(t)$ . A typical plot of  $\beta(t)$  vs t obtained after a step increase in interfacial area of ca. 10% is shown in Figure 13, also shown is the fitted decay using a double exponential. Both the double and triple exponentials were found to fit the data well but for simplicity, the double exponential was used for subsequent analysis. The decay curves all showed the same general behavior, with an initially rapid decay over short times leading to a longer timescale decay before returning to the equilibrium value. Larger initial increases of around 1-1.2 mNm<sup>-1</sup> in interfacial tension were seen with the 2k PEO star polymer compared to the 5k PEO polymer where the increases were of the order of 0.6 mNm<sup>-1</sup>, in agreement with the trend seen in the moduli obtained from the oscillatory tests.

The fitted double-exponential relaxation curves were Fourier transformed by numerically integrating eqs 8 and 9 in Excel. The integrations were carried out over the whole of the experimental data for a series of discrete frequencies from  $1 \times 10^{-5}$  to 0.2 Hz. The Nyquist–Shannon theorem for signal

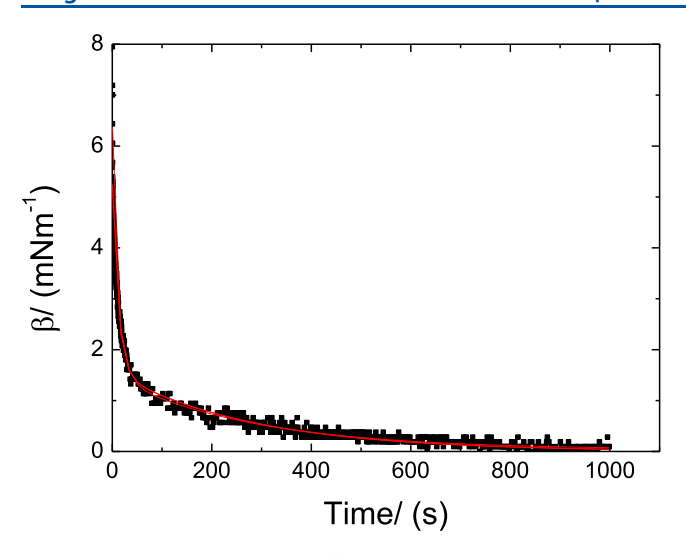


Figure 13. Relaxation plot of  $\beta(t)$  vs t for 0.2% 5k PEO at the n-dodecane/water interface. The solid line is a double-exponential decay fit.

processing shows that for a continuous signal comprising equal spaced signals at time interval t, the highest frequency that is

fully described by that function is 1/2t in Hertz. <sup>67,68</sup> The time interval used in the analysis of the decay function was 0.2 s, and so the theoretical highest frequency would be 2.5 Hz. However, it was found that the interfacial tension took a finite time to settle down after the droplet expansion due to a short-lived oscillation caused by rapid expansion. This time was typically of the order of 0.5 s, which corresponds to a frequency of 2 rad·s<sup>-1</sup> or 0.32 Hz, and to minimize any errors a maximum frequency of 0.2 Hz was chosen for the upper limit.

The moduli vs frequency plots obtained from the Fourier transforms of the interfacial tension decay function are shown in Figure 14 for all four polymers (0.2%)/oil phase combinations, also plotted are the moduli obtained from the oscillation measurements. The fitting parameters for the double-exponential fit are listed in Table 2. All fittings with the double-exponential showed regression coefficient  $(R^2)$  values of 0.95 or better.

Two distinct relaxation times were obtained for each of the four polymer/oil pairings, the shorter being in the range 3.1–6.9 s and the longer in the range 278–384 s. The relative strengths of the two relaxation peaks can be assessed by the ratios of the pre-exponential factors ( $A_1$  and  $A_2$  referring to the shorter and longer relaxation times, respectively). The value of

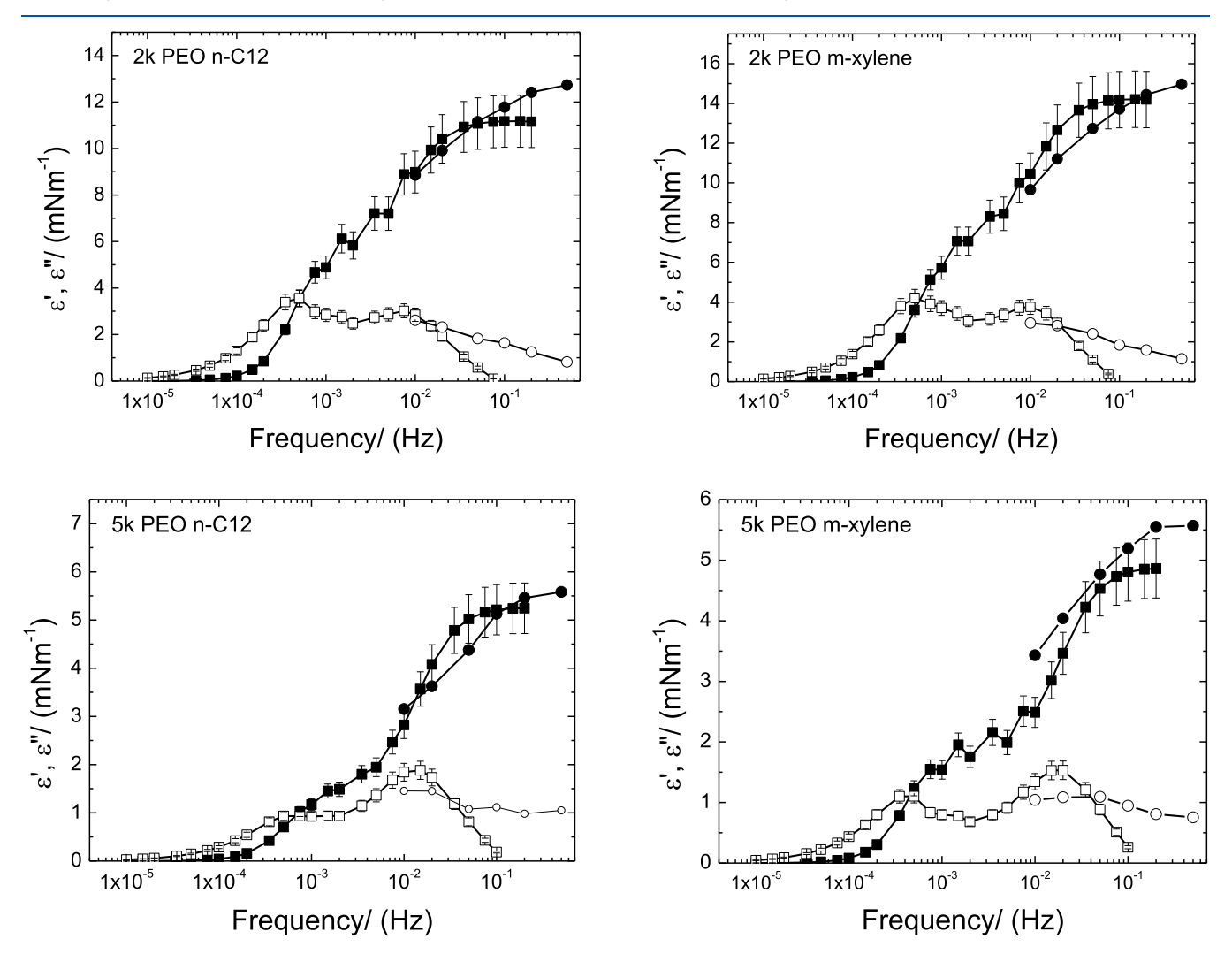


**Figure 14.** Frequency dependence of the interfacial moduli for the four polymer/oil pairing obtained using interfacial relaxation ( $\blacksquare$ - $\varepsilon'$ ,  $\square$ - $\varepsilon''$ ). The data are also compared to the moduli obtained from the oscillation measurements at the higher frequencies ( $\varepsilon'$ - $\blacksquare$ ,  $\varepsilon''$ - $\bigcirc$ ).

Table 2. Fitted Parameters of a Double-Exponential Fitting of the Decay Functions Arising from ca. 10% Dilations of Preequilibrated Adsorbed Layers of Star Polymers at the Oil/Water Interface at an Aqueous Polymer Concentration of 0.2%

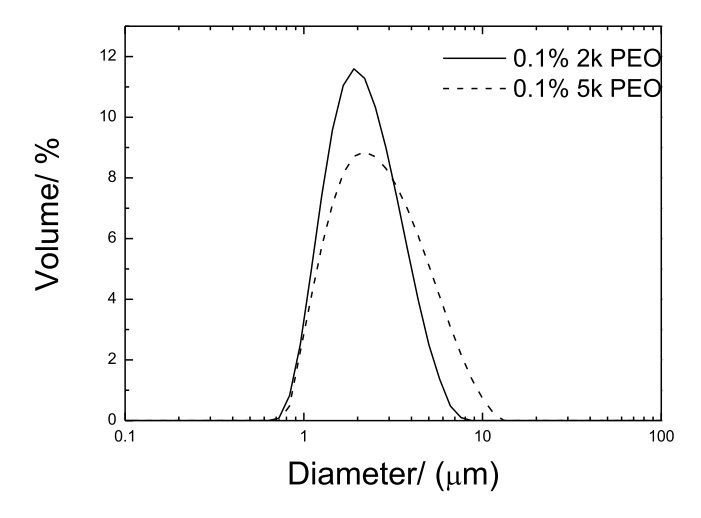
$_{M_{n}}^{\mathrm{PEO}}$	oil phase	$A_1$	$t_1$	$A_2$	$t_2$	$A_1/A_2$	$R^2$
2k	n-dodecane	5.39	18.97	6.18	345.2	0.87	0.97
2k	m-xylene	6.93	14.38	7.61	292.2	0.91	0.98
5k	n-dodecane	3.76	11.58	1.57	278.8	2.39	0.98
5k	m-xylene	3.12	8.54	1.94	384.1	1.61	0.95

 $A_1/A_2$  was larger with the 5k PEO star than that with m-xylene showing the short-time relaxation process was the dominant one at the higher molecular weight. The ratio for the 2k PEO star was roughly half that seen with the 5k PEO being close to one with both oils showing that both relaxation processes were of roughly equal importance.

The frequency sweeps for all four pairs generated from the relaxation data reflect the two relaxation processes seen in the relaxation data, with two apparent peaks in the loss moduli. The elastic moduli for all four systems show reasonable agreement with the oscillatory data (0.01-0.5 Hz) although the loss moduli show poorer agreement. Both the 2k and 5k PEO analogues reached apparent plateaus between 0.01 and 0.1 Hz with the elastic moduli falling down to zero as the frequency was reduced. As seen in the oscillation measurements, the higher-frequency elastic modulus was most dependent on the PEO arm molecular weight, with the 2k PEO star plateau modulus being between 11 and 14 mNm<sup>-1</sup> compared to the 5 mNm<sup>-1</sup> achieved by the 5k PEO star with both oils. The loss modulus also showed differences between the two polymer analogues corresponding to the two relaxation times identified from the analysis of the relaxation curves. The 5k PEO star showed a dominant peak between 0.01 and 0.02 Hz with both oils corresponding to the short-time relaxation process and at longer times (in the region of  $5 \times 10^{-4}$  Hz) a hump or a weak peak. In the case of the 2k PEO star, the higher-frequency peak was between 0.005 and 0.01 Hz, while the low frequency was also at  $5 \times 10^{-4}$  Hz.

The relaxation process seen at around 0.01 Hz was responsible for the collapse of the data when the frequency was normalized to  $c^{-2}$  in the oscillation data and was primarily a result of the desorption/adsorption of particles. On this timescale, the adsorbed particles have sufficient interfacial mobility as a result of the interfacial area increase to allow polymer particles to move around the interface and make room for additional particles. This results in surprisingly facile adsorption of particles as the system returns to equilibrium and a diffusion-controlled relaxation. The relaxation process at longer times is likely to reflect changes in the conformation or arrangement of the adsorbed polymers at the interface. In this region, the particles are approaching equilibrium adsorbed concentrations and the closer packing requires more cooperative movement and potentially a change in the conformation of polymer chains to accommodate any further particles to finally achieve the equilibrium interfacial excess. The magnitude of the longer time relaxation peak is lower with the higher-molecular-weight 5k PEO star polymer, suggesting this process is more facile with the softer interactions, lower interfacial pressure, and likely lower packing of these particles than for the lower-molecular-weight 2k PEO star allowing the bulk of the relaxation to occur over a shorter timescale. The relative conformational freedom of the longer EO chains resulting from their greater length and marginally lower density of arms (16.7 per molecule compared to 24.7 for the 2k sample) gives them greater surface mobility than the more densely packed harder 2k particles. This lower surface mobility of the 2k PEO system leads to a slower relaxation and a more pronounced peak in the loss spectrum at low frequencies.

The ultrasonic emulsification of n-dodecane into the 0.2% dispersions of 2k PEO and 5k PEO star in water yielded o/w emulsions with broadly similar initial droplet sizes of 2.2 and 2.8  $\mu$ m, respectively, with the 2k PEO polymer producing emulsions with a narrower droplet size distribution (Figure 15). The small difference in interfacial tension between the 2k and 5k PEO stars at the n-dodecane/water interface would have contributed to the slightly lower size seen with the 2k PEO star, but this contribution would be small. The difference in droplet size was more likely to be due to the short-time stabilizing effect of the adsorbed particles (i.e., rates of transport and adsorption at freshly formed interfaces).



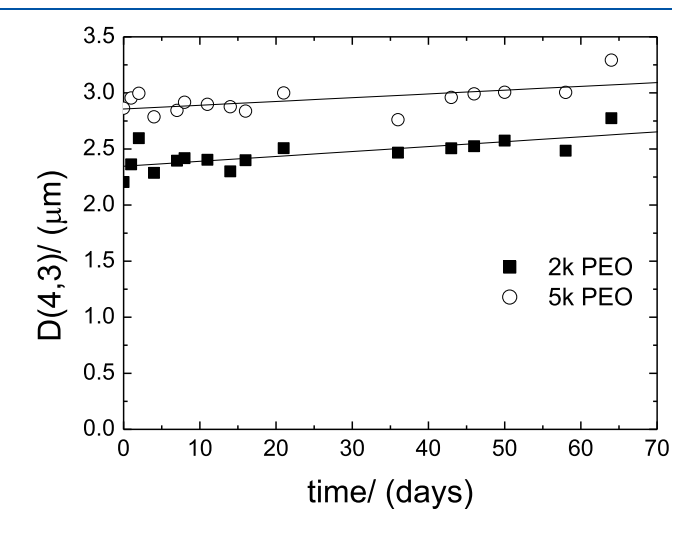
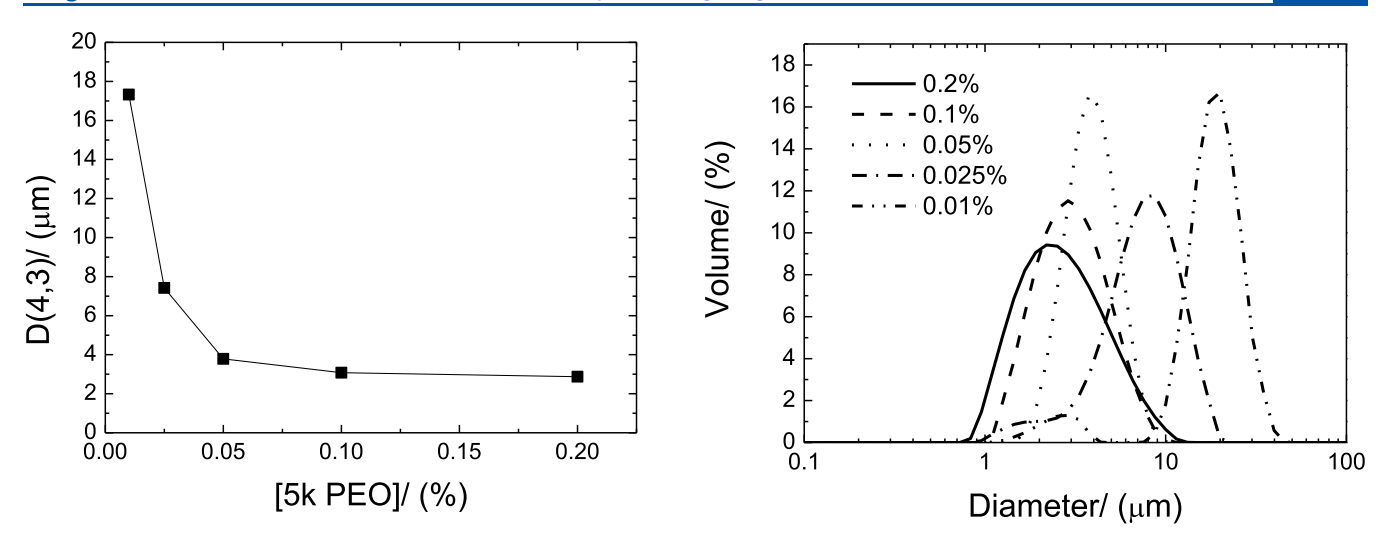


Figure 15. (Left) Initial droplet volume distributions of the emulsions formed and (right) evolution of the volume mean diameter of the emulsion droplets with time during storage at 20 °C.



**Figure 16.** (Left) Initial volume mean diameter of the *n*-dodecane in water emulsion droplets as a function of 5k PEO star polymers in the aqueous phase and (right) initial volume distributions of the emulsions at various aqueous concentrations of 5k PEO star in the aqueous phase.

Neither emulsion showed any great instability in terms of droplet growth over a period of 60 days despite the fact that the elastic interfacial modulus of the 2k PEO at the *n*-dodecane/water interface is almost twice that of the 5k PEO system. Linear regression of the D(4, 3) vs time plots (Figure 15) gave growth rates of  $4.4 \times 10^{-3}$  and  $3.4 \times 10^{-3}$   $\mu$ m/day; these are not significantly different. Both polymers produced stable emulsions that showed little growth and no liberation of free oil over the entire storage period.

The effect of the concentration of 5k PEO star polymers on the volume diameter of 10% v/v n-dodecane emulsions is shown in Figure 16. The mean droplet size was dependent on the concentration of the polymer with the size showing a sharp initial decrease with increasing polymer concentration at low concentrations. However, the droplet size stabilized at around 0.05%, and essentially became independent of concentration. This behavior of droplet size and stabilizer concentration is often seen in Pickering stabilized systems. The droplet size is a competition between the droplet size attainable by the power input of the mechanical homogenizer and the interfacial area that the particles present in the system can effectively cover. At low concentrations, the homogenizing energy is capable of producing small droplets, but these have a larger interfacial area than the particles can fully cover, and thus the droplet size tends to be larger as the partly coated small droplets undergo some limited coalescence as they are not effectively stabilized. At a high particle concentration, the total area that the particles may cover is larger than that produced by the homogenizer, and so the droplet size is purely controlled by the energy of the homogenizer and the droplet size becomes independent of particle concentration.

Plots of the mean diameter as a function of time (Figure 17) show that there was little difference in the rate of growth of the droplets at the various 5k PEO star polymer concentrations. The rate of increase all lay in the range of  $2.2 \times 10^{-3} - 1.75 \times 10^{-2} \ \mu \text{m/day}$  for 0.2 down to 0.025% polymer, and the changes were of the same order of magnitude as the error in the measurement, and so any differences can only be taken as an indication that the emulsion stability was not strongly dependent on the polymer concentration. However, free oil was seen to be liberated within 1 week of preparation in n-dodecane emulsions containing 0.01% 5k PEO. The stability

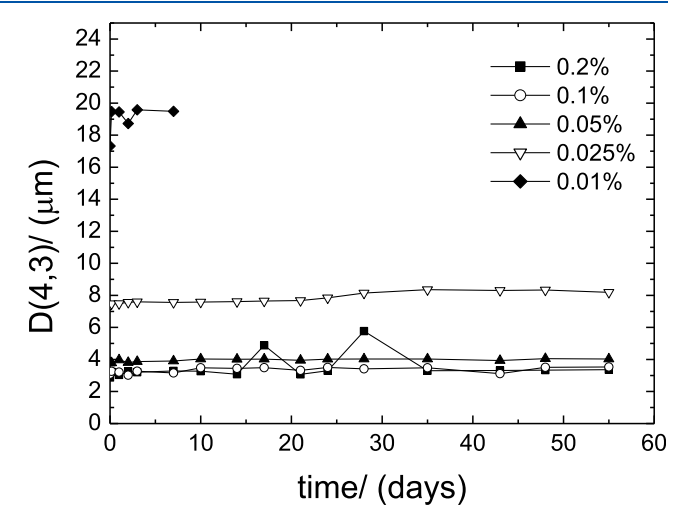


Figure 17. Time evolution of the volume diameter (D(4, 3)) of *n*-dodecane in water emulsions stabilized by 5k PEO star polymers at aqueous concentrations in the range 0.01-0.02%.

seen at all concentrations (except 0.01%) suggests that an effective interfacial barrier to coalescence is formed even at low concentrations, in agreement with previous studies on star polymer-stabilized emulsions. 31,34-36 The interfacial tension for the 5k PEO against *n*-dodecane was essentially independent of concentration suggesting that the adsorbed interfacial excess was also independent of concentration. Georgieva et al. suggested that in terms of emulsion stability, the low-frequency elastic interfacial modulus was a factor in the stability toward Ostwald ripening, whereas that at high frequency was important in preventing or reducing coalescence.<sup>52</sup> Coalescence may be thought of as being the result of localized thinning of the film between adjacent droplets causing the two droplets to touch and so coalesce. As mentioned earlier, the presence of a significant dilatational modulus can cause Marangoni flows that tend to resist this thinning.<sup>53</sup> The localized thinning is the result of short-time thermal fluctuations of the interface and so relates to the elastic moduli at high frequencies. The collapse of the oscillatory data for different concentrations onto single curves shows that the high-frequency moduli will be independent of concentration,

and this would lead to the stability being independent of concentration. It should be noted that the concentration of free polymer will be lower than the total amount in the system as a result of adsorption at the interface, but it would appear that, other than at 0.01%, the remaining free polymer was sufficiently high to maintain the interfacial properties at a sufficiently high level to stabilize the emulsions.

The results obtained shed some new light on the nature of the adsorption of star polymers with low grafting densities of arms at the oil/water and the air/water interfaces. The dynamic surface tension data suggested that the adsorption of the polymers at the air/water interface was diffusion-controlled and dependent on the square of the concentration of the polymer in the aqueous phase. It was unexpected that the same conclusion could be drawn from the interfacial rheology data. Conventional wisdom suggests that adsorbed particles are essentially irreversibly adsorbed at the interface due to the high adsorption energies involved. The free energy of adsorption,  $\Delta G$ , is given by  $^{41}$ 

$$\Delta G = \pi r^2 \gamma_{\text{ow}} (1 + |\cos \theta_{\text{w}}|)^2 \tag{13}$$

where r is the particle radius,  $\gamma_{\rm ow}$  is the interfacial tension, and  $\theta_{\rm w}$  is the equilibrium three-phase contact angle.

Many Pickering emulsions reported in the literature are stabilized by particles that are 50 nm or larger leading to high free energies of adsorption; however, the star polymers are much smaller and should have significantly lower values. The reason underlying the high adsorption energy is that the clean interface between an immiscible oil and water will show a high interfacial free energy. When a particle is adsorbed, the unfavorable clean interfacial area is replaced by two new interfaces, particle/oil and particle/water. For an effective Pickering stabilizer, each of these interfaces will be much less energetic since the particles will have a greater affinity for both the oil and the water than the oil has for the water. The free energy difference between the clean interface and the replacement two interfaces arising from the particle adsorption is very large, leading to a very strongly adsorbed particle. The free energy term is essentially the energy required to transfer a particle from the interface to either of the bulk phases (depending on which phase wets the particle more effectively, this is the origin of the need for the modulus of the cosine). An optimum particle would have a contact angle of 90° for the particle in either phase, and at this point, the free energy is at maximum. 41 A reduction in the contact angle of the particle in either aqueous or oil phase reduces the energy of transfer into that phase, weakening the adsorption.

The area of the adsorbed particle is relatively well defined for solid uniform particles, but this is not the case for star polymers with a hydrophobic core and grafted hydrophilic arms. The hydrophobic cores of the 2k PEO and the 5k PEO stars were 2.6 and 2.4 nm. respectively. Taking the 5k PEO core radius as being representative for the two, a plot of the free energy of adsorption as a function of contact angle is shown in Figure 18 at both the *n*-dodecane/water and the *m*-xylene interfaces (taking the average measured interfacial tensions of 26.7 and 17.5 mNm<sup>-1</sup>, respectively). The lower interfacial tension between m-xylene and water (37 mNm<sup>-1</sup>) compared to that of n-dodecane and water (52 mNm<sup>-1</sup>) demonstrates the lower hydrophobicity of the aromatic oil. This is reflected in the interfacial tensions at the two interfaces and in the free of adsorption energies calculated for the two

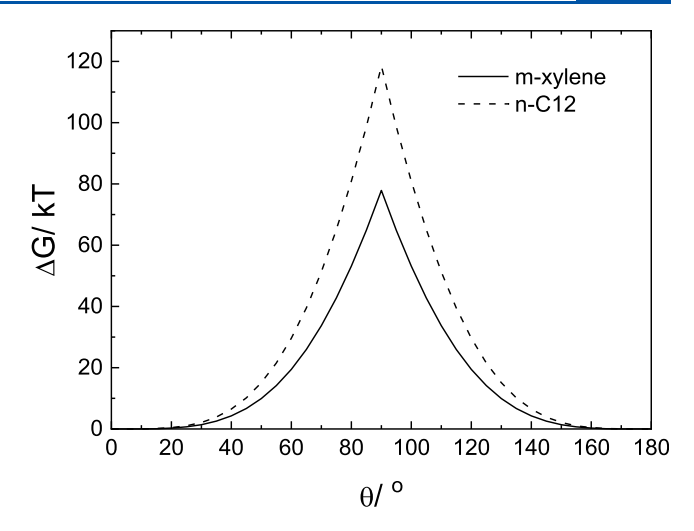


**Figure 18.** Free energy of adsorption calculated for the hydrophobic cores alone at the *m*-xylene/water and the *n*-dodecane/water interfaces.

oils with the adsorption of the polymer core at the m-xylene/ water interface being lower than for the n-dodecane. Due to the small size of the core, the free energy of adsorption is relatively low compared to many Pickering systems. The threephase contact angles are unknown in these systems, for an unmodified pDVB particle, the contact angle would be relatively high. However, the presence of the grafted chains, despite being present at a low grafting density, would reduce the contact angle to some extent leading to a reduced adsorption energy. Zell et al. 72 have studied the desorption of linear PEO at different molecular masses under compression and reported a desorption energy of 0.15 kT per monomer at the air/ water interface, which is similar to an estimated value 0.4 kT per monomer given by Bjisterbosch et al.<sup>73</sup> using polymer scaling analysis. This suggests that the adsorption energy at the oil/ water interface of the PEO arms on the star polymers would contribute little to any adsorption/desorption. The main contribution of the PEO arms will be in their effect on the water contact angle on the polymer core as well as their relative solubilities in the aqueous and oil phases.

For contact angles below 35-40°, the free energies obtained for the cores alone were 4 kT or less, which would allow relatively facile adsorption/desorption during droplet dilation. However, higher contact angles up to 90° would be expected to be sufficient to provide a strong adsorption to the interface compared to thermal energy, so disfavoring desorption during the compression stage of the dilation process. The energy of adsorption of the whole molecule will be further significantly modified by the presence of the hydrophilic arms and their interactions with the aqueous phase and the oil phase. Venohr reported a Flory-Huggins parameter for PEO in bulk water of  $\chi = 0.45$ , showing the great affinity for the polymer in water.<sup>74</sup> Galin reported values for PEO in *n*-dodecane of  $\chi = 2.1-2.7$ and for PEO in p-xylene (which is expected to be similar to mxylene) of  $\chi = 0.38-0.44$ . It should be noted that Galin's values were for 70 °C; however, they demonstrate the overall difference in solvency of the two solvents for PEO. Due to the lack of solubility of the PEO arms in n-dodecane and greater solubility in the aqueous phase, their presence will cause the adsorbed polymers to reside to a greater extent in the aqueous phase thus reducing the contact angle. The 5k PEO arms will draw the particles further into the aqueous phase to a greater

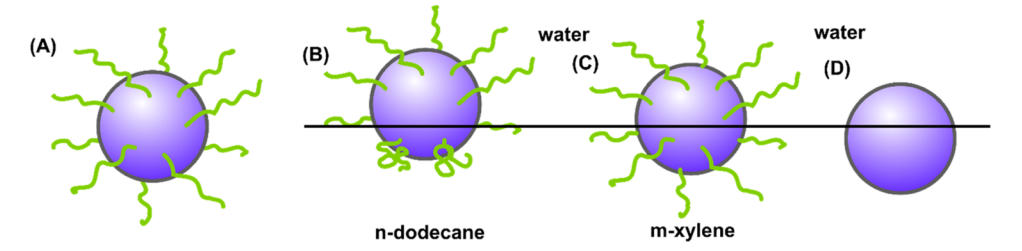


**Figure 19.** Schematic depiction of the 5k PEO star (A) in water alone (B) at the *n*-dodecane /water interface with collapsed PEO chains in the oil phase and (C) at the *m*-xylene/water interface with more extended PEO chains in the oil and (D) for a bare pDVB particle at either oil/water interface. Note the greater penetration of the polymer core into the *m*-xylene compared to the *n*-dodecane and the greater collapse of PEO chains in *n*-dodecane compared to those in *m*-xylene. Not to scale.

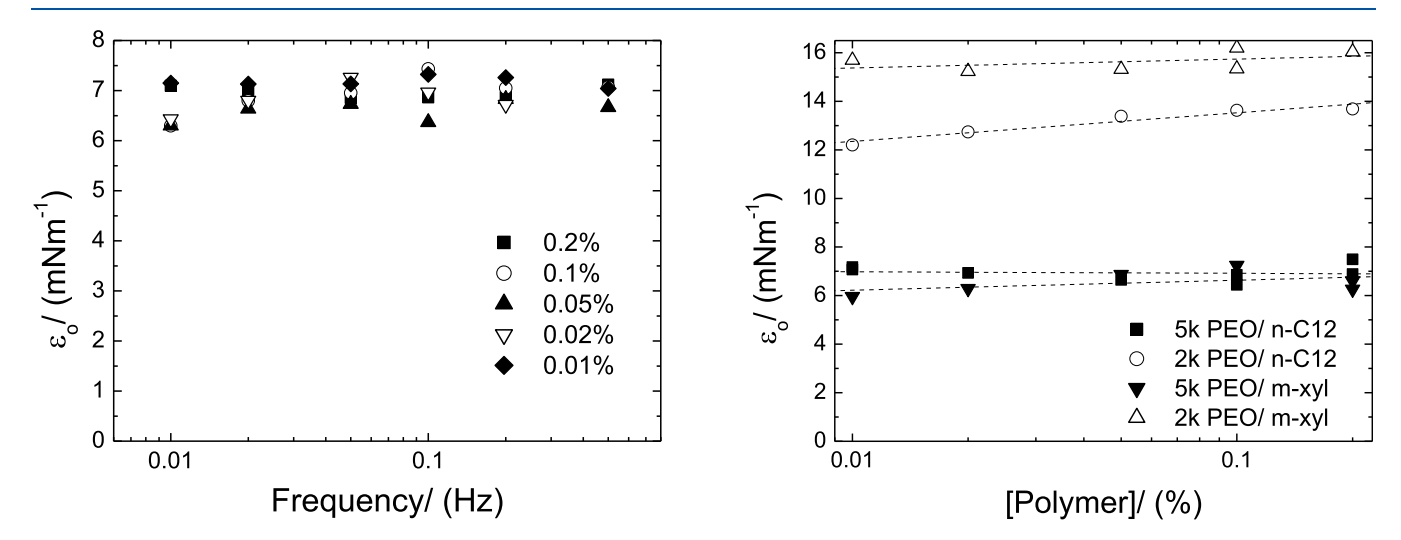


**Figure 20.** (Left) Variation in limiting interfacial modulus,  $\varepsilon_{o}$ , with frequency for the 5k PEO star polymer at the dodecane/water interface. (Right) Variation in the average limiting interfacial modulus with concentration for the four polymer/oil combinations.

extent than the 2k PEO, despite the greater grafting density of the latter. This effect also reduces the amount of PEO that is directly interacting with the oil phase. This will not necessarily be the case for adsorption at the water/m-xylene interface since the m-xylene will show a greater affinity for the pDVB core than the aliphatic n-dodecane and the PEO arms have greater solubility in the *m*-xylene and the polymer core will sit more in the oil phase compared to a bare pDVB particle; this is shown schematically in Figure 19 for the 5k PEO star. Overall, to greater or lesser extents, the effect of the hydrophilic chains will be to moderate the penetration of the cores into the interface and so reduce the contact angle and the free energy of adsorption. This facilitates the adsorption/desorption during the oscillatory dilation leading to frequency-dependent interfacial moduli. It also accounts for the variation seen in the kinetics of the interfacial tension. The slower approach to equilibrium seen with the 2k PEO star compared to the 5k PEO star results from the greater penetration of the hydrophobic core into the interface. This would appear to be the rate-determining step for this length of PEO arm since 2k PEO stars showed the same kinetics at both m-xylene and ndodecane/water interface despite the difference in arm solubility in the oil. Thus, the star polymers may be considered as being intermediate between a particle and a polymer when adsorbing at an interface.

Zell et al. studied the desorption of 8.4 nm diameter iron oxide nanoparticles stabilized by 2.5k and 5k PEO with ca. 170 and 140 arms per particle.<sup>72</sup> They found that despite desorption energies of 1160 kT with 2.5k PEO arms and

1930 kT with 5k PEO arms, the particles were able to desorb under sufficient surface pressure. These values are surprisingly high to allow desorption, but they suggest that desorption/ adsorption of star polymers is not unrealistic.

It is useful to compare this treatment to star polymers with higher graft densities of 2k PEO arms since the greater density of PEO arms would be expected, on the basis of the argument proposed above, to result in systems that showed weak adsorption and highly frequency-dependent interfacial moduli. However, as mentioned earlier, similar polymers with 64 arms showed the opposite effect in which the moduli at comparable concentrations were independent of frequency. Moreover, polymers with 460 arms showed nonsinusoidal interfacial tension responses during oscillatory dilation. This was attributed to molecules being ejected under compression and suggested that they acted very much as particles. Lee et al. 16 studied adsorbed layers (at the air/ water interface) of the polymer brush poly(ethylene oxide)-poly(*n*-butyl acrylate) using neutron reflectivity and surface pressure-area isotherms. The results showed that water is a poorer solvent for the grafted PEO arms compared to free PEO in water. They reported that the Flory-Huggins interaction parameter for the grafted chains in water was  $\chi = 0.79 - 0.85$  compared to the better than theta value of  $\chi = 0.45$  for free PEO in water. This reduced solubility and hydration of grafted PEO chains in water would be most pronounced for monomer units closest to the core where they are most closely packed and less pronounced toward the periphery of the polymer. This would suggest that as the PEO grafting density increases, the

hydrophobic core effectively becomes larger. Thus, the polymer becomes increasingly particle-like, so accounting for the apparently stronger adsorption of the 64 and 460 2k PEO arm polymers with graft densities of 1 and 0.54 nm² per arm, compared to the 3.6 nm² per arm of the 2k PEO star. The desorption energy found by Zell<sup>68</sup> for iron oxide nanoparticles of similar core size to the pDVB core polymers was much higher. The reason for this may again be due to the high graft density (ca. 1.3–1.6 arms/nm²) effectively reducing the solubility of the PEO arms effectively increasing the core size and rendering the particle more hydrophobic.

The normalization of the frequency by  $c^2$  suggested that the rheology was diffusion-controlled and that the star polymers could readily adsorb and desorb during oscillation. A further test may be applied to the frequency data, in that in the case of a diffusion-controlled interfacial response the limiting or high-frequency interfacial modulus,  $\varepsilon_{\rm o}$ , is independent of frequency since it is the equilibrium value and is dependent only on the concentration. For a diffusion-controlled process,  $\varepsilon_{\rm o}$  is given by  $^{73}$ 

$$\varepsilon_{\rm o} = \frac{\varepsilon^{'2} + \varepsilon^{''2}}{\varepsilon' - \varepsilon''} \tag{14}$$

A representative plot of  $\varepsilon_{\rm o}$  as a function of frequency is shown in Figure 20 for 5k PEO star at the waer/n-dodecane interface. The modulus is essentially independent of frequency confirming that the interfacial modulus is governed by a diffusional process. Similar frequency-independent behavior was seen with all four polymer/oil phase pairings. Moreover, the limiting modulus (averaged over the individual values at each frequency) was independent of concentration for each of the four polymer/oil combinations (Figure 20) showing that the adsorbed layer was similar for all concentrations.

# CONCLUSIONS

Star polymers with 2k and 5k PEO arms at relatively low grafting density adsorbed at air/water and oil/water interfaces show interesting properties at the oil/water interface. The properties of the adsorbed layer were dependent on the nature of the oil phase, with lower interfacial tensions seen at the mxylene/water interface compared to that at the n-dodecane/ water interface. The molecular weight of the PEO arms had only a small effect on the magnitude of interfacial tensions and interfacial pressure for each of the two oil phases, while the rate of approach to equilibrium tension was dependent on the molecular weight of PEO arms. Oscillatory and relaxationbased interfacial rheology measurements were powerful techniques in the understanding of the adsorbed layers of star polymers at the o/w interface. Both methods showed that the adsorbed layers of particles were viscoelastic, becoming increasingly elastic at lower concentrations. The data obtained as a function of frequency and concentration suggests that, surprisingly, the particles could adsorb and desorb on the timescale of the oscillation used in the measurements and that the characteristic timescale for this process was controlled by  $1/c^2$ . This concentration dependence was also seen in the adsorption of the particles at the air/water interface and their effect on the dynamic surface tension. Emulsion stability tests showed that despite a relatively facile adsorption/desorption to and from the interface, the star polymer particles were effective emulsion stabilizers.

#### ASSOCIATED CONTENT

# Supporting Information

The Supporting Information is available free of charge at https://pubs.acs.org/doi/10.1021/acs.langmuir.3c00557.

Repeat plots of interfacial moduli ( $\varepsilon'$  and  $\varepsilon''$ ) vs frequency for two polymer/oil systems (0.1% 5k PEO star/n-dodecane and 0.1% 2k star PEO vs m-xylene) showing variability between measurements, and plots of interfacial moduli ( $\varepsilon'$  and  $\varepsilon''$ ) and phase angle ( $\phi$ ) vs frequency for 2k PEO star vs n-dodecane, 5k PEO star vs n-dodecane and 5k PEO star vs m-xylene (PDF)

# AUTHOR INFORMATION

# **Corresponding Authors**

Krzysztof Matyjaszewski — Department of Chemistry, Carnegie Mellon University, Pittsburgh, Pennsylvania 15213, United States; orcid.org/0000-0003-1960-3402; Email: km3b@andrew.cmu.edu

Philip Taylor — Syngenta, Jealott's Hill International Research Centre, Bracknell, Berkshire RG42 6EY, U.K.; oorcid.org/ 0000-0003-1182-7719; Email: Phil.taylor@syngenta.com

# **Authors**

Mateusz Olszewski – Department of Chemistry, Carnegie Mellon University, Pittsburgh, Pennsylvania 15213, United States

Xiaolei Hu − Department of Chemistry, Carnegie Mellon University, Pittsburgh, Pennsylvania 15213, United States Ting-Chih Lin − Department of Chemistry, Carnegie Mellon University, Pittsburgh, Pennsylvania 15213, United States; orcid.org/0000-0003-3665-1203

Natalia Lebedeva – Syngenta Crop Protection, LLC, Greensboro, North Carolina 27409, United States

Complete contact information is available at: https://pubs.acs.org/10.1021/acs.langmuir.3c00557

#### Notes

The authors declare no competing financial interest.

# ACKNOWLEDGMENTS

Financial support from NSF (DMR 2202747) is gratefully acknowledged. The authors thank Syngenta for permission to publish this work.

# REFERENCES

- (1) Aveyard, R.; Binks, B. P.; Clint, J. H. Emulsions stabilised solely by colloidal particles. *Adv. Colloid Interface Sci.* **2003**, *100*–*102*, 503–546.
- (2) Saleh, N.; Phenrat, T.; Sirk, K.; Dufour, B.; Ok, J.; Sarbu, T.; Matyjaszewski, K.; Tilton, R. D.; Lowry, G. V. Adsorbed triblock copolymers deliver reactive iron nanoparticles to the oil/water interface. *Nano Lett.* **2005**, *5*, 2489–2494.
- (3) Saigal, T.; Dong, H.; Matyjaszewski, K.; Tilton, R. D. Pickering Emulsions Stabilized by Nanoparticles with Thermally Responsive Grafted Polymer Brushes. *Langmuir* **2010**, *26*, 15200–15209.
- (4) Zhou, J.; Qiao, X.; Binks, B. P.; Sun, K.; Bai, M.; Li, Y.; Liu, Y. Magnetic Pickering emulsions stabilized by Fe3O4 nanoparticles. *Langmuir* **2011**, *27*, 3308–3316.
- (5) Chevalier, Y.; Bolzinger, M.-A. Emulsions stabilized with solid nanoparticles: Pickering emulsions. *Colloids Surf., A* **2013**, 439, 23–34.

- (6) Ridel, L.; Bolzinger, M. A.; Gilon-Delepine, N.; Dugas, P. Y.; Chevalier, Y. Pickering emulsions stabilized by charged nanoparticles. *Soft Matter* **2016**, *12*, 7564–7576.
- (7) Zhang, T.; Xu, J.; Chen, J.; Wang, Z.; Wang, X.; Zhong, J. Protein nanoparticles for Pickering emulsions: A comprehensive review on their shapes, preparation methods, and modification methods. *Trends Food Sci. Technol.* **2021**, *113*, 26–41.
- (8) Dworakowska, S.; Lorandi, F.; Gorczyński, A.; Matyjaszewski, K. Toward Green Atom Transfer Radical Polymerization: Current Status and Future Challenges. *Adv. Sci.* **2022**, *9*, No. 2106076.
- (9) Matyjaszewski, K. Advanced Materials by Atom Transfer Radical Polymerization. *Adv. Mater.* **2018**, *30*, No. 1706441.
- (10) Matyjaszewski, K. Atom Transfer Radical Polymerization (ATRP): Current Status and Future Perspectives. *Macromolecules* **2012**, *45*, 4015–4039.
- (11) Matyjaszewski, K.; Xia, J. Atom Transfer Radical Polymerization. Chem. Rev. 2001, 101, 2921-2990.
- (12) Morell, M.; Voit, B.; Ramis, X.; Serra, A.; Lederer, A. Synthesis, characterization, and rheological properties of multiarm stars with poly(glycidol) core and poly(methyl methacrylate) arms by AGET ATRP. J. Polym. Sci., Part A: Polym. Chem. 2011, 49, 3138–3151.
- (13) Venkatesh, R.; Staal, B. B. P.; Klumperman, B.; Monteiro, M. J. Characterization of 3- and 4-Arm Stars from Reactions of Poly(butyl acrylate) RAFT and ATRP Precursors. *Macromolecules* **2004**, *37*, 7906–7917.
- (14) Jankova, K.; Bednarek, M.; Hvilsted, S. Star polymers by ATRP of styrene and acrylates employing multifunctional initiators. *J. Polym. Sci., Part A: Polym. Chem.* **2005**, 43, 3748–3759.
- (15) Zhang, Y.; Fu, L.; Li, S.; Yan, J.; Sun, M.; Giraldo, J. P.; Matyjaszewski, K.; Tilton, R. D.; Lowry, G. V. Star Polymer Size, Charge Content, and Hydrophobicity Affect their Leaf Uptake and Translocation in Plants. *Environ. Sci. Technol.* **2021**, *55*, 10758–10768.
- (16) Gao, H.; Matyjaszewski, K. Synthesis of functional polymers with controlled architecture by CRP of monomers in the presence of cross-linkers: From stars to gels. *Prog. Polym. Sci.* **2009**, *34*, 317–350.
- (17) Lutz, J.-F.; Neugebauer, D.; Matyjaszewski, K. Stereoblock Copolymers and Tacticity Control in Controlled/Living Radical Polymerization. *J. Am. Chem. Soc.* **2003**, *125*, 6986–6993.
- (18) Wang, Y.; Matyjaszewski, K. Hairy nanoparticles by atom transfer radical polymerization in miniemulsion. *React. Funct. Polym.* **2022**, *170*, No. 105104.
- (19) Min, K.; Gao, H.; Yoon, J. A.; Wu, W.; Kowalewski, T.; Matyjaszewski, K. One-Pot Synthesis of Hairy Nanoparticles by Emulsion ATRP. *Macromolecules* **2009**, *42*, 1597–1603.
- (20) Silverstein, M. S.; Shach-Caplan, M.; Bianco-Peled, H.; Tsarevsky, N. V.; Cooper, B. M.; Matyjaszewski, K. Nanoscale structure of SAN-PEO-SAN triblock copolymers synthesized by ATRP. *PMSE Prepr.* **2006**, *95*, 172–173.
- (21) Angot, S.; Murthy, K. S.; Taton, D.; Gnanou, Y. Atom Transfer Radical Polymerization of Styrene Using a Novel Octafunctional Initiator: Synthesis of Well-Defined Polystyrene Stars. *Macromolecules* **1998**, *31*, 7218–7225.
- (22) Gao, H.; Matyjaszewski, K. Synthesis of Star Polymers by A New "Core-First" Method: Sequential Polymerization of Cross-Linker and Monomer. *Macromolecules* **2008**, *41*, 1118–1125.
- (23) Gao, H.; Matyjaszewski, K. Arm-First Method As a Simple and General Method for Synthesis of Miktoarm Star Copolymers. *J. Am. Chem. Soc.* **2007**, *129*, 11828–11834.
- (24) Gao, H.; Matyjaszewski, K. Synthesis of Miktoarm Star Polymers via ATRP Using the \"In-Out\" Method: Determination of Initiation Efficiency of Star Macroinitiators. *Macromolecules* **2006**, 39, 7216–7223.
- (25) Gao, H.; Matyjaszewski, K. Synthesis of Star Polymers by a Combination of ATRP and the \"Click\" Coupling Method. *Macromolecules* **2006**, *39*, 4960–4965.
- (26) Gao, H.; Matyjaszewski, K. Structural Control in ATRP Synthesis of Star Polymers Using the Arm-First Method. *Macromolecules* **2006**, *39*, 3154–3160.

- (27) Gao, H.; Tsarevsky, N. V.; Matyjaszewski, K. Synthesis of Degradable Miktoarm Star Copolymers via Atom Transfer Radical Polymerization. *Macromolecules* **2005**, 38, 5995–6004.
- (28) Francis, R.; Lepoittevin, B.; Taton, D.; Gnanou, Y. Toward an Easy Access to Asymmetric Stars and Miktoarm Stars by Atom Transfer Radical Polymerization. *Macromolecules* **2002**, *35*, 9001–9008
- (29) Whittaker, M. R.; Urbani, C. N.; Monteiro, M. J. Synthesis of 3-Miktoarm Stars and 1st Generation Mikto Dendritic Copolymers by "Living" Radical Polymerization and "Click" Chemistry. J. Am. Chem. Soc. 2006, 128, 11360–11361.
- (30) Saigal, T.; Riley, J. K.; Golas, P. L.; Bodvik, R.; Claesson, P. M.; Matyjaszewski, K.; Tilton, R. D. Poly(Ethylene Oxide) Star Polymer Adsorption at the Silica/Aqueous Interface and Displacement by Linear Poly(Ethylene Oxide). *Langmuir* **2013**, *29*, 3999–4007.
- (31) Li, W.; Yu, Y.; Lamson, M.; Silverstein, M. S.; Tilton, R. D.; Matyjaszewski, K. PEO-Based Star Copolymers as Stabilizers for Water-in-Oil or Oil-in-Water Emulsions. *Macromolecules* **2012**, *45*, 9419–9426.
- (32) Li, W.; Matyjaszewski, K. Uniform PEO Star Polymers Synthesized in Water via Free Radical Polymerization or Atom Transfer Radical Polymerization. *Macromol. Rapid Commun.* **2011**, 32, 74–81.
- (33) Li, W.; Matyjaszewski, K. Star Polymers via Cross-Linking Amphiphilic Macroinitiators by AGET ATRP in Aqueous Media. *J. Am. Chem. Soc.* **2009**, *131*, 10378–10379.
- (34) Huang, Y.-R.; Lamson, M.; Matyjaszewski, K.; Tilton, R. D. Enhanced interfacial activity of multi-arm poly(ethylene oxide) star polymers relative to linear poly(ethylene oxide) at fluid interfaces. *Phys. Chem. Phys.* **2017**, *19*, 23854–23868.
- (35) Xie, G.; Krys, P.; Tilton, R. D.; Matyjaszewski, K. Heterografted Molecular Brushes as Stabilizers for Water-in-Oil Emulsions. *Macromolecules* **2017**, *50*, 2942–2950.
- (36) Saigal, T.; Yoshikawa, A.; Kloss, D.; Kato, M.; Golas, P. L.; Matyjaszewski, K.; Tilton, R. D. Stable emulsions with thermally responsive microstructure and rheology using poly(ethylene oxide) star polymers as emulsifiers. *J. Colloid Interface Sci.* **2013**, 394, 284–292.
- (37) Ramsden, W. Separation of solids in the surface-layers of solutions and 'suspensions' (observations on surface-membranes, bubbles, emulsions, and mechanical coagulation).—Preliminary account. *Proc. R. Soc. London* 1904, 72, 156–164.
- (38) Pickering, S. U. Emulsions. J. Chem. Soc., Trans. 1907, 91, 2001–2021.
- (39) Hunter, T. N.; Pugh, R. J.; Franks, G. V.; Jameson, G. J. The role of particles in stabilising foams and emulsions. *Adv. Colloid Interface Sci.* **2008**, *137*, 57–81.
- (40) Binks, B. P.; Lumsdon, S. O. Stability of oil-in-water emulsions stabilised by silica particles. *Phys. Chem. Chem. Phys.* **1999**, *1*, 3007–3016
- (41) Binks, B. P. Particles as surfactants—similarities and differences. Curr. Opin. Colloid Interface Sci. 2002, 7, 21–41.
- (42) Miller, R.; Fainerman, V. B.; Krägel, J.; Loglio, G. Surface rheology of adsorbed surfactants and proteins. *Curr. Opin. Colloid Interface Sci.* 1997, 2, 578–583.
- (43) Noskov, B. A.; Akentiev, A. V.; Bilibin, A. Y.; Zorin, I. M.; Miller, R. Dilational surface viscoelasticity of polymer solutions. *Adv. Colloid Interface Sci.* **2003**, *104*, 245–271.
- (44) Langevin, D.; Monroy, F. Interfacial rheology of polyelectrolytes and polymer monolayers at the air—water interface. *Curr. Opin. Colloid Interface Sci.* **2010**, *15*, 283–293.
- (45) Bos, M. A.; van Vliet, T. Interfacial rheological properties of adsorbed protein layers and surfactants: a review. *Adv. Colloid Interface Sci.* **2001**, 91, 437–471.
- (46) Freer, E. M.; Yim, K. S.; Fuller, G. G.; Radke, C. J. Interfacial Rheology of Globular and Flexible Proteins at the Hexadecane/Water Interface: Comparison of Shear and Dilatation Deformation. *J. Phys. Chem. B* **2004**, *108*, 3835–3844.

- (47) Hsieh, T.-L.; Martinez, M. R.; Garoff, S.; Matyjaszewski, K.; Tilton, R. D. Interfacial dilatational rheology as a bridge to connect amphiphilic heterografted bottlebrush copolymer architecture to emulsifying efficiency. *J. Colloid Interface Sci.* **2021**, *581*, 135–147.
- (48) Liggieri, L.; Attolini, V.; Ferrari, M.; Ravera, F. Measurement of the Surface Dilational Viscoelasticity of Adsorbed Layers with a Capillary Pressure Tensiometer. *J. Colloid Interface Sci.* **2002**, 255, 225–235.
- (49) Hansen, F. K. Surface Dilatational Elasticity of Poly(oxy ethylene)-Based Surfactants by Oscillation and Relaxation Measurements of Sessile Bubbles. *Langmuir* **2008**, 24, 189–197.
- (50) Alvarez, N. J.; Anna, S. L.; Saigal, T.; Tilton, R. D.; Walker, L. M. Interfacial Dynamics and Rheology of Polymer-Grafted Nanoparticles at Air—Water and Xylene—Water Interfaces. *Langmuir* **2012**, 28, 8052–8063.
- (51) Chan, D. H. H.; Hunter, S. J.; Neal, T. J.; Lindsay, C.; Taylor, P.; Armes, S. P. Adsorption of Sterically-Stabilized Diblock Copolymer Nanoparticles at the Oil-Water Interface: Effect of Charged End-Groups on Interfacial Rheology. *Soft Matter* **2022**, *18*, 6757–6770.
- (52) Georgieva, D.; Schmitt, V.; Leal-Calderon, F.; Langevin, D. On the Possible Role of Surface Elasticity in Emulsion Stability. *Langmuir* **2009**, *25*, 5565–5573.
- (53) Lucassen-Reynders, E. Interfacial viscoelasticity in emulsions and foams. *Food Struct.* **1993**, *12*, No. 1.
- (54) Manga, M. S.; Hunter, T. N.; Cayre, O. J.; York, D. W.; Reichert, M. D.; Anna, S. L.; Walker, L. M.; Williams, R. A.; Biggs, S. R. Measurements of Submicron Particle Adsorption and Particle Film Elasticity at Oil—Water Interfaces. *Langmuir* **2016**, *32*, 4125–4133.
- (55) Botti, T. C.; Hutin, A.; Quintella, E.; Carvalho, M. S. Effect of interfacial rheology on drop coalescence in water—oil emulsion. *Soft Matter* **2022**, *18*, 1423—1434.
- (56) Yarranton, H. W.; Sztukowski, D. M.; Urrutia, P. Effect of interfacial rheology on model emulsion coalescence: I. Interfacial rheology. *J. Colloid Interface Sci.* **2007**, *310*, 246–252.
- (57) Yarranton, H. W.; Urrutia, P.; Sztukowski, D. M. Effect of interfacial rheology on model emulsion coalescence: II. Emulsion coalescence. *J. Colloid Interface Sci.* **2007**, *310*, 253–259.
- (58) Wang, J.-S.; Matyjaszewski, K. Controlled/"living" radical polymerization. atom transfer radical polymerization in the presence of transition-metal complexes. *J. Am. Chem. Soc.* **1995**, *117*, 5614–5615
- (59) Matyjaszewski, K.; Miller, P. J.; Pyun, J.; Kickelbick, G.; Diamanti, S. Synthesis and Characterization of Star Polymers with Varying Arm Number, Length, and Composition from Organic and Hybrid Inorganic/Organic Multifunctional Initiators. *Macromolecules* 1999, 32, 6526–6535.
- (60) Lorandi, F.; Fantin, M.; Matyjaszewski, K. Atom Transfer Radical Polymerization: A Mechanistic Perspective. *J. Am. Chem. Soc.* **2022**, *144*, 15413–15430.
- (61) Corrigan, N.; Jung, K.; Moad, G.; Hawker, C. J.; Matyjaszewski, K.; Boyer, C. Reversible-deactivation radical polymerization (Controlled/living radical polymerization): From discovery to materials design and applications. *Prog. Polym. Sci.* **2020**, *111*, No. 101311.
- (62) Matyjaszewski, K.; Jakubowski, W.; Min, K.; Tang, W.; Huang, J.; Braunecker, W. A.; Tsarevsky, N. V. Diminishing catalyst concentration in atom transfer radical polymerization with reducing agents. *Proc. Natl. Acad. Sci. U.S.A.* **2006**, *103*, 15309–15314.
- (63) Jakubowski, W.; Matyjaszewski, K. Activators regenerated by electron transfer for atom-transfer radical polymerization of (meth)-acrylates and related block copolymers. *Angew. Chem., Int. Ed.* **2006**, 45, 4482–4486.
- (64) Xia, J.; Matyjaszewski, K. Controlled/\"Living\" Radical Polymerization. Atom Transfer Radical Polymerization using Multidentate Amine Ligands. *Macromolecules* 1997, 30, 7697–7700.
- (65) Aveyard, R.; Haydon, D. A. Thermodynamic properties of aliphatic hydrocarbon/water interfaces. *Trans. Faraday Soc.* **1965**, *61*, 2255–2261.

- (66) Monteux, C.; Fuller, G. G.; Bergeron, V. Shear and Dilational Surface Rheology of Oppositely Charged Polyelectrolyte/Surfactant Microgels Adsorbed at the Air—Water Interface. Influence on Foam Stability. *J. Phys. Chem. B* **2004**, *108*, 16473—16482.
- (67) Loglio, G.; Tesei, U.; Cini, R. Spectral data of surface viscoelastic modulus acquired via digital fourier transformation. *J. Colloid Interface Sci.* **1979**, *71*, 316–320.
- (68) Loglio, G.; Rillaerts, E.; Joos, P. Fourier transform surface viscoelastic modulus of dilute aqueous solutions of surfactants. Improved computational methods. *Colloid Polym. Sci.* **1981**, 259, 1221–1227.
- (69) Kitching, S.; Johnson, G. D. W.; Midmore, B. R.; Herrington, T. M. Surface Rheological Data for a Polymeric Surfactant Using a Pulsed Drop Rheometer. *J. Colloid Interface Sci.* **1996**, *177*, 58–69.
- (70) Ferri, J. K.; Stebe, K. J. Which surfactants reduce surface tension faster? A scaling argument for diffusion-controlled adsorption. *Adv. Colloid Interface Sci.* **2000**, *85*, 61–97.
- (71) Freer, E. M.; Wong, H.; Radke, C. J. Oscillating drop/bubble tensiometry: effect of viscous forces on the measurement of interfacial tension. *J. Colloid Interface Sci.* **2005**, 282, 128–132.
- (72) Zell, Z. A.; Isa, L.; Ilg, P.; Leal, L. G.; Squires, T. M. Adsorption Energies of Poly(ethylene oxide)-Based Surfactants and Nanoparticles on an Air—Water Surface. *Langmuir* **2014**, *30*, 110–119.
- (73) Bijsterbosch, H. D.; de Haan, V. O.; de Graaf, A. W.; Mellema, M.; Leermakers, F. A. M.; Stuart, M. A. C.; van Well, A. A. Tethered Adsorbing Chains: Neutron Reflectivity and Surface Pressure of Spread Diblock Copolymer Monolayers. *Langmuir* **1995**, *11*, 4467–4473.
- (74) Venohr, H. F. V.; Strunk, H.; Borchard, W. Static and Dynamic Light Scattering from Aqueous Poly(ethylene oxide) Solutions. *Eur. Polym. J.* **1998**, 34, 723–732.
- (75) Galin, M. Gas-liquid chromatography study of poly(ethylene oxide)-solvent interactions: estimation of polymer solubility parameter. *Polymer* **1983**, *24*, 865–870.
- (76) Lee, H.; Kim, D. H.; Witte, K. N.; Ohn, K.; Choi, J.; Akgun, B.; Satija, S.; Won, Y.-Y. Water Is a Poor Solvent for Densely Grafted Poly(ethylene oxide) Chains: A Conclusion Drawn from a Self-Consistent Field Theory-Based Analysis of Neutron Reflectivity and Surface Pressure—Area Isotherm Data. J. Phys. Chem. B 2012, 116, 7367—7378.